Towards calibration-free solid-contact ion-selective electrodes: study and improvement of the standard potential stability

Åbo Akademi University

Faculty of Science and Engineering

Jay Pee P. Oña

Master's programme in Excellence in Analytical Chemistry

Degree project in Analytical chemistry, 30 credits

Supervisor: Dr. Zekra Mousavi (Åbo Akademi University)

Cosupervisor(s): Docent Dr. Tomasz Sokalski (Åbo Akademi University)

Dr. Kim Granholm (Åbo Akademi University)

Prof. Ivo Leito (University of Tartu)

August 2018

Preface

This master's thesis was performed at the Laboratory of Analytical Chemistry, Åbo Akademi University, under the Erasmus Mundus joint master's program, EACH (Excellence in Analytical Chemistry).

First, my sincerest thanks to Professor Johan Bobacka for encouraging us to pursue research in applied electrochemistry and paving the way for our future academic careers. Thank you for your body of work in this important field and your patient guidance.

My deep gratitude to my main thesis supervisor, Dr. Zekra Mousavi, for her endless patience and guiding hands throughout the course of this work. To Dr. Tomasz Sokalski and Dr. Kim Granholm for your valuable advice and supervision, thank you very much.

To Professor Ivo Leito for giving me this incredible opportunity to become part of the EACH program. And to Miss Ülle Tensing for her most valued assistance during one of the most challenging times of my life. I will be forever grateful.

To all my friends and colleagues in the EACH program, whom I have shared some of my most joyful moments, thank you very much.

And most of all to my family, my fountain of strength and joy, thank you and I love you the most.

Åbo, August 2018

Jay Pee Permejo Oña

Table of contents

Preface ..... **ii**

Table of contents ..... **iii**

List of symbols ..... **v**

List of abbreviations ..... **vi**

1. Introduction **1**

2. Potentiometric ion sensors **2**

2.1. Principles of potentiometric measurements 3

2.2. Solid-contact Ion-selective electrodes 5

2.3. Electrically conducting polymers 7

2.4. Poly(3,4-ethylenedioxythiophene) 8

2.5. Ion-selective membrane 9

2.6. Stability of standard potential, E^o 11

2.7. Characterization techniques 13

2.7.1 Cyclic voltammetry 13

2.7.2 Potentiometry 14

2.7.3. Electrochemical impedance spectroscopy 15

2.7.4. Energy dispersive analysis of X-ray 16

3. Experimental Procedure **16**

3.1. Chemicals 16

3.2. Electrochemical synthesis of PEDOT(PSS) and PEDOT(Cl) 17

3.2.1. Electrode preparation and modification 17

3.2.2. Galvanostatic polymerization of PEDOT(PSS) and PEDOT(Cl) 18

3.3. Fabrication of solid-contact K^+-ISEs 18

3.4. Fabrication of solid-contact Cl^--ISEs 18

3.5. Cyclic Voltammetry (CV) Measurements 19

3.6. Electrochemical impedance spectroscopy (EIS) 19

3.7. Chronopotentiometry 20

3.8. Potentiometric measurements 20

3.9. Scanning electron microscopy (SEM)/ energy dispersive analysis of X-ray (EDAX) 20

4. Results and discussion **21**

4.1. Characterization of solid-contact K^+-ISEs and evaluation of E^o stability 21

4.1.1. Cyclic voltammetry (CV) measurements 21

4.1.2. Potentiometric measurements 22
4.1.3. Electrochemical Impedance Spectroscopy (EIS) 24
4.1.4. Chronopotentiometry 26
4.1.5. Evaluation of E^o stability 28
4.2. Electrochemical properties of GC/PEDOT(PSS) conditioned in 0.01 M $AgNO_3$ 33
4.2.1. Cyclic voltammetry measurements 33
4.2.2. SEM/EDAX measurements 34
4.2.3 Potentiometric measurements 36
4.3. Assessment of E^o stability of K^+-ISEs with Ag-deposited PEDOT(PSS) films as solid-contact 40
4.4. Characterization of solid-contact Cl^--ISEs and assessment of E^o stability 43
4.4.1. CV and EIS measurements 43
4.4.2. Potentiometric measurements 44
4.4.3. Chronopotentiometry 46
4.4.4. Evaluation of E^o stability 48
5. Conclusions 52
6. References 54
7. Appendix 57

List of symbols

ac	alternating current
a_i	activity of species *i*
a_j	activity of interfering ion *j*
C_{LF}	low-frequency capacitance
dc	direct current
E	measured potential
E_{cell}	cell potential
E_{ind}	indicator electrode potential
E_j	liquid junction potential
E^o	standard potential
E_{ref}	reference electrode potential
F	Faraday's constant
f	frequency
i	applied current
Kij	selectivity coefficient for primary ion *i* over interfering ion *j*
R_T	total resistance
R	universal gas constant (8.314 J/mol*K)
Z	impedance
z_i	charge of species i
z_j	charge of species j
γ	activity coefficient
ω	angular frequency
φ	phase shift

List of abbreviations

Ag	silver
Au	gold
AuNPs	gold nanoparticles
CV	cyclic voltammetry
CWE	coated wire electrode
DOS	bis(2-ethylhexyl)sebacate
ECP	electrically conducting polymer
EDAX	energy dispersive analysis of X-ray
EDOT	3,4-ethylenedioxythiophene
EIS	electrochemical impedance spectroscopy
GC	glassy carbon
GC-AuNPs	gold nanoparticles-modified glassy carbon
ISE	ion-selective electrode
ISM	ion-selective membrane
KTpClPB	potassium tetrakis(4-chlorophenyl)borate
LiOAc	lithium acetate
NE	Nikolskii-Eisenman
o-NPOE	2-nitrophenyl octyl ether
PEDOT	poly(3,4-ethylenedioxythiophene)
PPy	polypyrrole
PSS	poly(styrenesulfonate)
Pt	platinum
PVC	poly(vinyl chloride)
RE	reference electrode
SC-ISE	solid-contact ion-selective electrode
SEM	scanning electron microscopy
TDMACl	tridodecylmethylammonium chloride
THF	tetrahydrofuran

1. Introduction

Potentiometric ion sensors or ion-selective electrodes (ISEs) are widely used in routine analytical measurements as well as in clinical applications due to their selectivity, fast response and relatively low-cost. However, in order to be used in more demanding analytical applications such as on-line process analysis and remote sensing, ion-selective electrodes must be robust and maintenance-free. One approach towards this objective is the development of all-solid-state ion-selective electrodes without any internal filling solution. Solid-state ion-selective electrodes based on conducting polymers have been extensively studied in recent years [1]. The unique electrochemical properties of conducting polymers make them attractive materials for ion-to-electron transduction in solid-contact ISEs (SC-ISEs).

An important prerequisite for obtaining reliable potentiometric ion sensors is high potential stability. For ISEs with solid-contact, Nikolskii and Materova [2] identified three conditions that must be fulfilled to obtain stable electrode potentials: (1) Reversible and stable transitions from ionic to electronic conductivity, (2) High exchange current which must be greater than the current passed during measurement, and (3) Absence of side reactions which occur alongside the main electrode reaction. As earlier demonstrated by Bobacka [3], ion-selective electrodes with doped poly(3,4-ethylenedioxythiophene) (PEDOT) as solid-contact material fulfill stability conditions 1-3 mainly due to the high bulk (redox) capacitance of the conducting polymer.

Despite the impressive properties and proven advantages of SC-ISEs based on conducting polymers, they still have not been integrated into commercial devices for practical use. In order to achieve this, SC-ISEs must match or surpass the performance of conventional liquid-contact ISEs. One of the limitations of SC-ISEs is the stability of measured potentials in between calibrations. Although reproducible slopes have been achieved using SC-ISEs, the quality of SC-ISEs is better assessed from the reproducibility of the standard potentials (E^o) [4].

In order to improve the stability of E^o, various studies have been made to find suitable materials to meet the requirements for potential stability and enhance the ion-to-electron transduction. These include the study of different dopants for conducting polymers and the incorporation of metal clusters (e.g. Au or Ag) into the polymer film to increase conductivity

[5]. The electron-conducting substrates also seem to affect the reproducibility of the standard potential [6]. Over the last two decades, nanomaterial modified electrodes have gained attention due to their high conductivity and signal amplification that are desirable for electroanalysis [7]. Among the currently available metal nanoparticles, gold nanoparticles are widely employed because of their large surface area, high electronic conductivity and good biocompatibility [7].

In this thesis, the long-term stability of solid-state ISEs is evaluated in terms of the reproducibility of their E^o over long periods. The data obtained in this work can provide an assessment of suitable materials which can be used to produce calibration-free ISEs. The context of a calibration-free ISE in this case refers to a sensor which does not require frequent calibrations. PEDOT is used as solid-contact material due to its high stability and high conductivity in its p-doped state. The effect of using different dopants for PEDOT and the deposition of silver (Ag) on the PEDOT(PSS) film towards E^o stability are assessed. Furthermore, the effect of using gold nanoparticles-modified glassy carbon (GC-AuNPs) electrode as conducting substrate on the long-term stability is studied.

2. Potentiometric ion sensors

The desire to monitor all aspects of environment, industry, human health and safety gave rise to the development of devices called sensors. Sensors are measuring devices that transform an input signal based on the property to be quantified into an output signal transmitted and registered by some instrument [8]. Sensors are generally divided into two types: physical sensors and chemical sensors. Physical sensors provide physical information of a system such as mass, pressure, temperature and humidity. On the other hand, chemical sensors transform chemical information, for example, concentration of a sample component, into an output signal [9].

A chemical sensor is composed of two essential parts: a receptor part and a transducer part. In the receptor part, the desired sample component or analyte selectively binds to a recognition layer through a physical, chemical or biochemical interaction. This process produces a form of energy that is measured in the transducer part which converts it into a useful measurable signal. This interaction is described in Figure 1. Depending on the operating

principle of the transducer, chemical sensors are classified as electrochemical, optical, mass and thermal sensors [9].

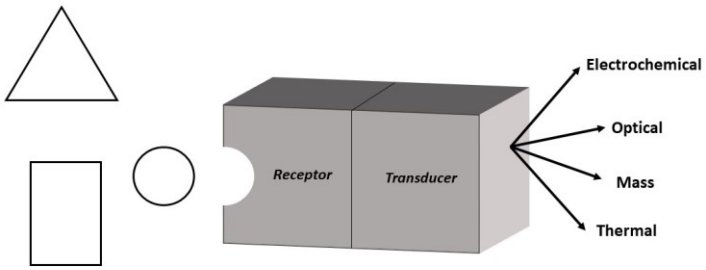

***Figure 1**. Schematic structure of a chemical sensor.*

Potentiometric ion sensors or ion-selective electrodes (ISEs) are a group of electrochemical sensors which yield a reversible electrode potential for a particular ionic species in solution. The potential of the electrode, measured against an appropriate reference electrode, is proportional to the logarithm of the activity of the analyte ion [10]. Such devices exhibit rapid response over a wide linear range, usually 1 to 10^{-6} M for most ISEs. Other features of ISEs such as their portability, low-energy consumption and low cost make them attractive for practical applications [11].

The selectivity of ISEs depends on the membrane which can be a glass or crystal membrane or a liquid ion-exchange material incorporated in a polymer matrix. The membrane is designed to generate a potential that is primarily due to the interaction with the ion of interest at the membrane-solution interface. Membrane materials with different ion-recognition capabilities have been developed to provide high selectivity. The main idea is to design membranes that will selectively bind the analyte and leave other ions in the solution [12].

2.1. Principles of potentiometric measurements

The equipment for a potentiometric measurement consists of an ion-selective electrode as indicator electrode and a reference electrode immersed in the same solution. The potential between the two electrodes is measured by a voltmeter with a high input impedance. The set-up for a potentiometric measurement using a conventional ISE is shown in Figure 2.

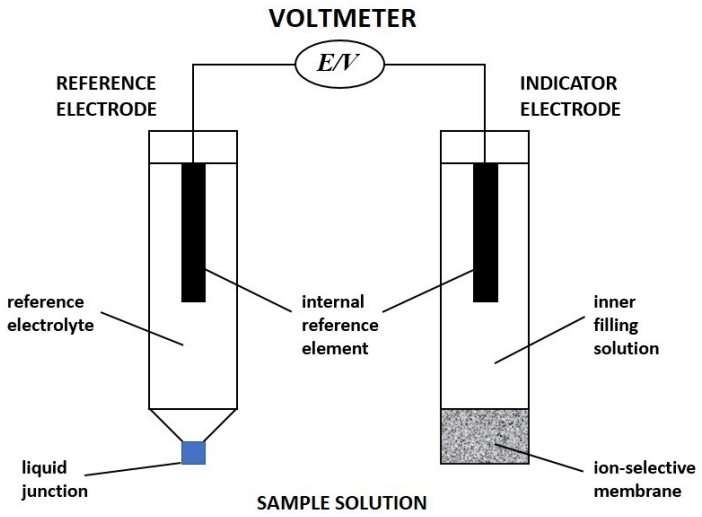

Figure 2. *Set-up of an electrochemical cell for potentiometric measurement*

The magnitude of the resulting potential depends on the potential difference between the ion-selective electrode and the reference electrode (E_{ind}-E_{ref}) and the liquid-junction potential (E_j) that develops at the interface of different solutions:

$$\boldsymbol{E_{cell} = E_{ind} - E_{ref} + E_j} \qquad \text{(Eq. 1)}$$

The potential of an ISE ideally obeys the Nernst equation (Eq. 2) which relates the cell potential and the activity of the target ion in the sample solution:

$$\boldsymbol{E = E^o + \frac{2.303RT}{z_iF} \log a_i} \qquad \text{(Eq. 2)}$$

where E is the measured potential, E^o is the standard potential, R is the universal gas constant, F is the Faraday's constant and T is the absolute temperature. a_i and z_i are activity and charge of the target ion, respectively [13]. The plot of E against the logarithm of ion activity a_i is a straight line with the slope corresponding to the magnitude ($2.303RT/z_iF$). For a monovalent cation (e.g. Ag^+) the potentiometric response would be cationic (Figure 3) and the slope would be equal to +59.2 mV/decade at 25°C as predicted by the Nernst equation. For a monovalent anion (e.g. Br^-) the potentiometric response would be anionic and the slope would be equal to -59.2 mV/decade (Figure 3) [14].

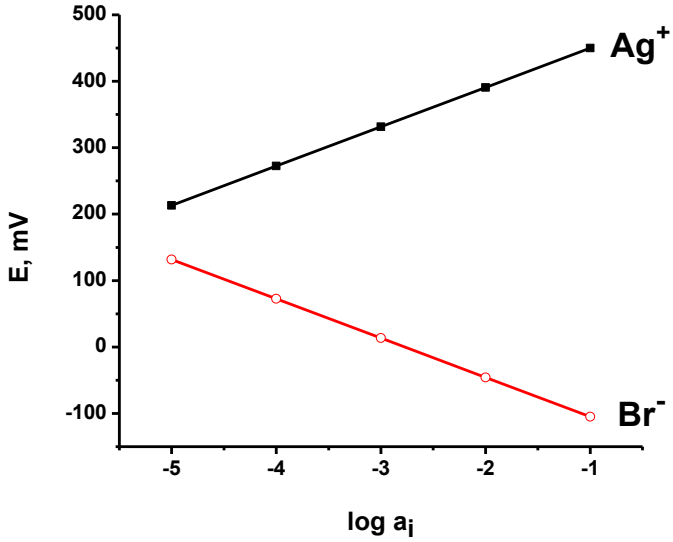

Figure 3. *Cationic response of ISE to a monovalent cation (Ag^+) and anionic response of ISE to a monovalent anion (Br^-)*

In most practical applications of ISEs the Nikolskii-Eisenman (NE) equation (Eq. 3) is used to take into account the effect of other ions present in the solution [11]:

$$E = E^o + Slog(a_i + \sum_{j \neq i}^{n} K_{ij}\, a_j^{z_i/z_j}) \qquad \text{(Eq. 3)}$$

where S is the slope of the calibration curve, K_{ij} is the selectivity coefficient, a_i is the activity of the primary ion (i), a_j is the activity of the interfering ion (j). z_i and z_j are the charges of the primary and interfering ion, respectively. The standard potential (E^o) can be experimentally obtained by taking the y-intercept of the linear part of the calibration curve.

2.2. Solid-contact Ion-selective electrodes

The construction of a conventional ISE as shown in Figure 2 consists of an ion-selective membrane, an internal reference element and an internal filling solution. The internal filling solution is prone to evaporation and sensitive to pressure and sample temperature. The need for more robust and easy to miniaturize ISEs gave rise to the development of solid-state ISEs. The invention of coated-wire electrode (CWE) in the 1970's was a big step in the development of all-solid-state ion selective electrodes [15]. The construction of CWE is shown in Figure 4a where the ion-selective membrane is directly attached to the conductive element. The

potential obtained from the CWE however was unstable due to blocked charge transfer and the poorly defined potential at the interface of the membrane and the electronically conducting substrate. An improved design included a solid intermediate layer between the membrane and the electronic conductor which can maintain a stable interfacial potential. This ISE construction (Figure 4b) was then known as solid-contact ion-selective electrode [16].

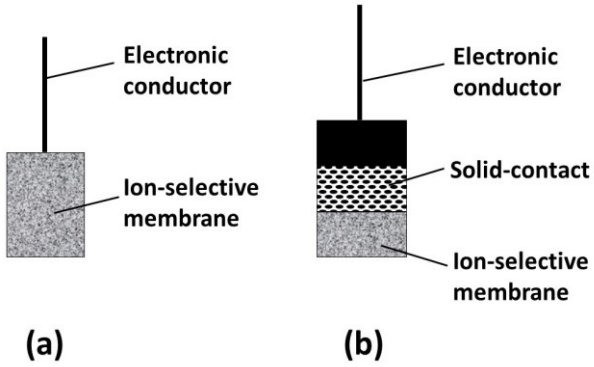

Figure 4. *Construction of coated-wire electrode (CWE) (a) and solid-contact ISE (b)*

The typical construction of a solid-contact ISE as shown in Figure 4b includes an electronic conductor (e.g. metal or glassy carbon), a solid-contact which allows a well-defined ion-to-electron transduction, and an ion-selective membrane (ISM) [16]. The ion-selective membrane is the most essential part of ISE as it determines the selectivity of the response to the target ion. One kind of ion-selective membrane is the solvent polymeric membrane which consists of a poly(vinyl chloride) (PVC) matrix and immobilized ion-carrier molecules called ionophores [17].

In order to replace the internal filling solution, the solid-contact must possess mixed electronic and ionic conductivity to serve as ion-to-electron transducer between the electronic conductor and the ion-selective membrane. Some electroactive conjugated polymers (electrically conducting polymers) were found to exhibit these properties and are now well studied ion-to-electron transducers for solid-contact ISEs [11].

2.3. Electrically conducting polymers

Electrically conducting polymers (ECPs) consist of a chain of carbon atoms connected by alternating single and double bonds forming a π-conjugated system. Figure 5 shows the molecular structures of two conducting polymers trans-polyacetylene and poly(3,4-ethylenedioxythiophene).

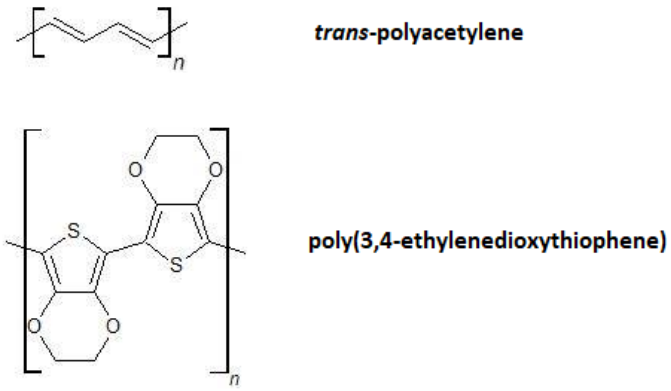

Figure 5. *Molecular structures of trans-polyacetylene and poly(3,4-ethylenedioxythiophene)*

Conducting polymers (CP) can be synthesized using chemical or electrochemical methods of polymerization. Chemical synthesis requires appropriate reagents and catalysts and is most suitable for mass production. Electrochemical polymerization is used when a thin polymer film is desired and good quality of the film is required [18]. The electrochemical method is the method of choice for many applications because it allows the control of film thickness by changing the potential or current with time [19].

Electrochemical polymerization can be done using three modes: constant potential (potentiostatic method), constant current (galvanostatic mode) and continuously varying potential (potentiodynamic method). In the potentiostatic method, the constant potential that is applied must be low-enough so that undesirable reactions do not occur but it should also allow the polymerization to proceed at a reasonable rate. The potentiostatic method also requires a separate coulometer to control the charge used for polymerization. In the galvanostatic method, the polymerization is forced to proceed at a constant current. The thickness of the film can then be controlled by adjusting the polymerization time. In the potentiodynamic method, continuously varying potentials are applied on the electrode during

the polymerization process. This method sometimes yields more stable and homogeneous film than when using the galvanostatic method [19].

The unusual conductive and optical properties of ECPs are due to the delocalization of π electrons along the polymer backbone. In the neutral (undoped) state, ECPs are insulators or semiconductors. To further increase the conductivity, ECPs are subjected to doping by removing electrons from (oxidation or p-doping) or adding electrons into (reduction or n-doping) the polymer film. Doping can be done chemically or electrochemically. In electrochemical doping, a proper potential is applied that will cause oxidation (electron removal) or reduction (electron addition) as shown below:

$$CP + A^- \rightarrow CP^+A^- + e^- \qquad \text{electrochemical p-doping (Eq. 4)}$$

$$CP + e^- + C^+ \rightarrow CP^-C^+ \qquad \text{electrochemical n-doping (Eq. 5)}$$

In the above equations, *CP* is the neutral form of the polymer, CP^+ and CP^- are the polymer's oxidized and reduced forms, respectively. A^- and C^+ represent the negative and positive counter ions. The extent of doping is controlled by the potential applied between the working electrode, where the polymer is deposited, and the reference electrode [20].

2.4. Poly(3,4-ethylenedioxythiophene)

Poly(3,4-ethylenedioxythiophene) (PEDOT) (Figure 5) belongs to a group of stable conducting polymers that have been extensively studied over the years as solid-contact for all-solid-state ion sensors [21]. PEDOT can be synthesized from its monomer, 3,4-ethylenedioxythiophene, using chemical or electrochemical polymerization. Chemical polymerization can be carried out using oxidizing agents such as iron(III) chloride ($FeCl_3$) or iron(III) p-toluenesulfonate ($Fe(OTs)_3$) [22]. Electrochemical polymerization of PEDOT can be done in aqueous solutions containing different types of doping anions, including chloride (Cl^-) and poly(styrene sulfonate) (PSS^-). The resulting PEDOT(Cl) or PEDOT(PSS) film is highly electroactive and very stable in the oxidized (p-doped) form [21]. The symmetry in cyclic voltammograms recorded for PEDOT films indicates high reversibility of the doping process which makes it a good candidate as an ion-to-electron transducer [23]. PEDOT(PSS) films have been used as ion-to-electron transducers for various ions including K^+, Ag^+ and Na^+ [11]. Solid-contact K^+-ISEs based on PEDOT showed

higher electrochemical stability in the presence of O_2 and CO_2 compared to SC-ISEs based on polypyrrole [23].

2.5. Ion-selective membrane

The ion-selective membrane provides the selectivity to a specific anion or cation. In most solid-contact ISEs, the ion-selective membrane consists of an ionophore embedded in a polymer matrix, a lipophilic salt and a plasticizer [24]. Ionophores are charged or neutral species that selectively binds the analyte ion. The selectivity of the analyte/ionophore association serves as the basis of the selectivity of the ISE [8]. A well-known ionophore is valinomycin which is often used in potassium selective membranes. The structure of valinomycin as shown in Figure 6 consists of twelve alternating amino acids and esters that form a macrocyclic molecule [17].

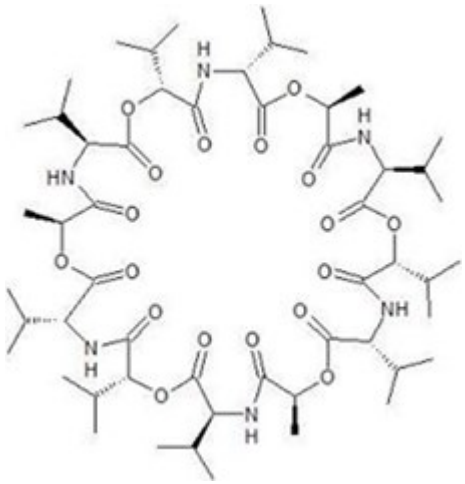

Figure 6. *Molecular structure of valinomycin* [17].

Valinomycin is able to form 1:1 complex with K^+ ions in solution through the interaction of the cation with the carbonyl oxygen atoms of the ester groups in the molecule. This results in a fast and reversible exchange of potassium ions in the sample solution. [17]

Lipophilic salts (ionic additives) are incorporated in the ion-selective membrane to provide permselectivity, or the ability to prevent the interference of counter ions (Donnan exclusion), and to reduce the electrical resistance of the membrane [25]. The lipophilic salt may dissociate into two lipophilic ions or into one lipophilic ion and one hydrophilic ion. In the latter case, the hydrophilic ion has the same charge as the analyte ion. As an example, for potassium-selective

ISEs, a small amount of potassium tetrakis(4-chlorophenyl)borate (KTpClPB) is added to the membrane cocktail. The lipophilic salt dissociates into the lipophilic tetrakis(4-chlorophenyl)borate anion and the hydrophilic potassium ion. The amount of lipophilic salt added must be carefully controlled as excessive concentrations can lead to drastic changes in the membrane selectivity [26].

The most common polymer matrix for ion-selective membranes is a plasticized polyvinyl chloride (PVC) which is composed of the polymer PVC and a plasticizer. A high molecular weight PVC is used to lessen the ionic contamination in the membrane. The plasticizer ensures the mobility of the free or complexed ionophore, sets the dielectric constant, and improves the mechanical properties of the membrane [27]. Two of the most common plasticizers are bis(2-ethylhexyl)sebacate (DOS) and 2-nitrophenyl octyl ether (o-NPOE). The chemical structures of DOS and o-NPOE are shown in Figure 7.

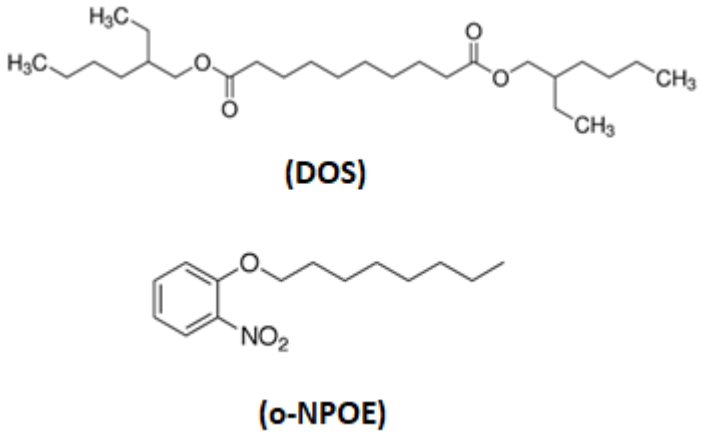

Figure 7. *Chemical structures of DOS and o-NPOE*

The typical composition of a PVC-based membrane contains 30-33% (wt.) PVC, 60-66% (wt.) plasticizer and 0.5-2 % (wt.) ionophore [8]. The molar ratio of the ionophore to the lipophilic salt is carefully optimized to improve the selectivity [28]. The components are dissolved in an organic solvent (e.g. tetrahydrofuran,THF) and the resulting mixture is referred to as the membrane cocktail. For SC-ISEs, an appropriate aliquot of the membrane cocktail is drop-cast directly on the substrate and allowed to dry, followed by suitable conditioning procedures [8].

2.6. Stability of standard potential, E^o

Despite the extensive research on ion-selective electrodes, obtaining ISEs with reproducible standard potential (E^o) remains a big challenge [11]. Lindner and Gyurcsányi pointed out that the quality of the solid-contact must be assessed by the reproducibility of the standard potentials and not just the response slopes [4]. Variations in E^o are often compensated by frequent calibrations but it must be stable and reproducible at least between two calibrations [29]. Reproducibility of E^o is essential for calibration-free, single use potentiometric ion sensors as well as sensors used for long-term monitoring (e.g. remote sensing) that require minimal calibration frequency [30].

In potentiometric measurements, the obtained potential difference between the reference electrode and the indicator electrode is affected by two components: the phase boundary potentials at all interfaces of the electrochemical cell, and the ohmic drop, V_{ohm}, which occurs between the two ends of any ionic or electrical conductor when a current is passed through it. V_{ohm} can be assumed to be very small as ion-selective potentiometry is almost always carried out in zero-current conditions. Therefore the potential measured is largely associated to the sum of all phase boundary potentials as illustrated in Figure 8 [28, 31].

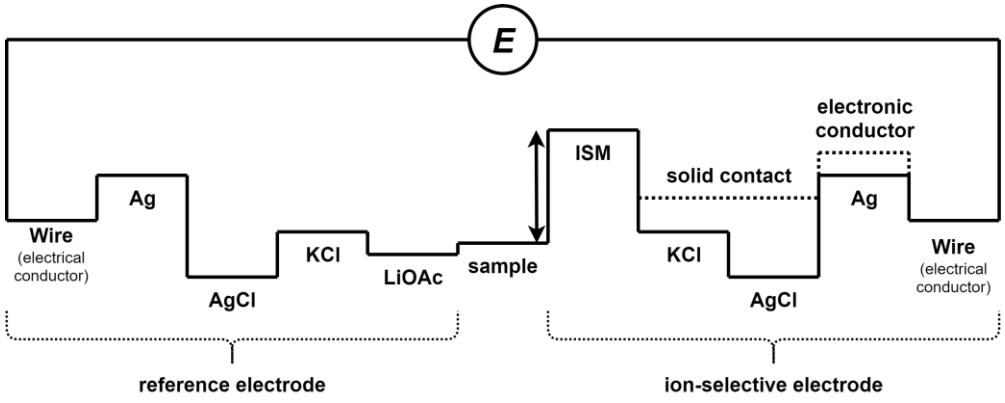

Figure 8. *Potential differences across the phase boundaries in an electrochemical cell constructed from a K^+-ISE and a reference electrode. The dashed lines represent the arrangement in a solid-state ISE* [31].

As the solid-contact, the potentials at the interfaces of the conducting polymer (CP) affect the overall potential of the SC-ISE system. These potentials are determined by the redox state and ion activities in the CP film and the composition of the phases the film is in contact with [32]. Ideally, if the CP potentials are stable, they can be incorporated into the E^o in Equation 3. However, CP potentials are affected by many factors including the dependence of the film

morphology on the polymerization process and the ability of counter ions to penetrate the film [30]. If the counter ion introduced into the polymer film during synthesis is small, this mobile anion (A^-) (i.e. in the case of p-doped CP) can move freely in and out of the polymer film during oxidation/reduction of the CP, as shown in Equation 6. On the other hand, if the counter anion is bulky (B^-), it is immobilized in the CP backbone and the negative charge can be compensated by small mobile cations (C^+). C^+ can move in and out of the polymer film when the CP is oxidized or reduced, as shown in Equation 7 [33].

$$(CP^+A^-)_{film} + e^- \rightleftharpoons (CP^0)_{film} + A^- \quad \text{(Eq. 6)}$$

$$(CP^+B^-)_{film} + C^+ + e^- \rightleftharpoons (CP^0B^-C^+)_{film} \quad \text{(Eq. 7)}$$

The stability of measured potentials in CP-based SC-ISEs is characterized by the potential drift that is unrelated to the concentration of the analyte in the samples tested. The potential stability of SC-ISEs is largely affected by the presence of polarizable interfaces, accumulation of water behind the ion-selective membrane (ISM) and the interference of light, CO_2 and O_2 [30]. In a study by Bobacka, it was observed that the potential stability depended on the capacitance of the CP as solid-contact, which is proportional to the thickness of the CP film used [3]. Furthermore, the capacitance of the CP can be enhanced by the dopant used, as demonstrated by Mousavi et al. for PEDOT doped with carbon nanotubes used as ion-to-electron transducer for K^+-ISE [34]. On the other hand, the formation of a water layer behind the ISM leads to drifting potentials, as the composition of the aqueous layer can be altered by the components in the sample [35]. Water accumulation is brought about by the inherent tendency of polymeric membranes to absorb water [8].

Several strategies to improve the stability and reproducibility of E^o of conducting polymer-based SC-ISEs have been reported. Vázquez et al. showed that a solution-cast film of PEDOT cross-linked with ruthenium redox couple ($Ru(NH_3)_6^{2+3+}$) improved the total bulk redox capacitance of PEDOT(PSS) and the E^o stability of the resulting K^+-ISE [36]. In a study conducted by Gyurcsányi et al., a K^+-ISE based on polypyrrole (PPy) doped with the redox pair hexacyanoferrate (II)/(III) used as a solid-contact showed lower potential drift than the K^+-ISE with hydrogel inner contact [37]. Lindfors et al. reported that Ca^{2+}-selective electrodes based

on the hydrophobic CP, poly(3-octylthiophene) as solid-contact showed lower standard deviation of E^o than a CWE-type Ca-ISE [38].

Conducting polymers with inclusions of metal particles has been studied in recent years for important applications such as catalysis of electrochemical reactions in low-temperature fuel cells and electrochemical sensors. An important feature of conducting polymer-metal composite materials is the stabilization of metal clusters by the nitrogen, oxygen and sulfur atoms in the polymer which prevents the aggregation of the metal. The resulting composite material has good porosity and high conductivity thus exhibiting good transport properties [5]. In an earlier work by Mousavi et al., it was observed that silver can be deposited in PEDOT and polypyrrole (PPy) films by simple conditioning in $AgNO_3$ solution [39]. The potentiometric sensors based on these $AgNO_3$-conditioned conducting polymers exhibited good sensitivity and selectivity towards Ag^+ ions.

Another important factor affecting the electrode potential of SC-ISEs is the nature of the electron conducting substrate (Figure 4b). In a recent study by Lindner et al., it was observed that the equilibration times of all-solid-state K^+-ISEs with the same solid-contact and ISM but with different conducting substrates (i.e., glassy carbon, Au, and Pt) were not similar. Results showed that electrodes built on glassy carbon and Au have shorter equilibration times than those with a Pt substrate [40]. It was also reported that reproducibility of E^o was better in electrodes with Au substrates than in identical electrodes with glassy carbon substrates [6]. The difference can be due to the variations in surface chemistry among different conducting substrates brought about by their intrinsic properties and the fabrication process [30].

2.7. Characterization techniques

2.7.1 Cyclic voltammetry

Cyclic voltammetry is a type of sweep technique in which the potential of an electrode is linearly scanned using a triangular waveform as shown in Figure 9. Throughout the potential scan, the current of the electrode is measured in an unstirred solution [14]. The cyclic voltammogram obtained can be used to study redox reactions of electroactive species. In the case of conducting polymers, cyclic voltammetry can either be used as a polymerization method or as a characterization tool for the synthesized polymers. It can give an estimate of

the charge-transfer rate in conducting polymers which may vary according to the morphology and chemical structure.

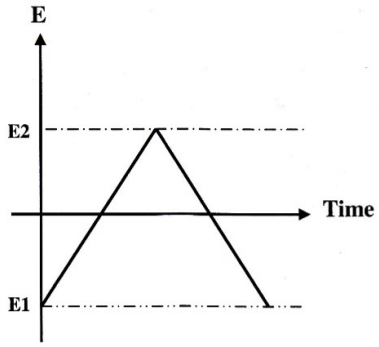

Figure 9. *Potential-time profile for cyclic voltammetry measurements* [14]

2.7.2 Potentiometry

For direct potentiometric measurements, the cell potential is the potential developed between the indicator electrode and the reference electrode. Ideally, the cell potential would correspond to the value of *E* given by the Nernst equation (Eq. 2). However, to account for the non-idealities of the indicator and reference electrodes, Eq. 2 can be written in the following form [8]:

$$E = L + S\log a_i \qquad \text{(Eq. 8)}$$

where the practical slope, $S = dE/d\log a_m$ and a_M is the activity of the ion *M*. For most metallic indicator electrodes, *L* is usually the standard potential (E^o) [13]. The activity of the ion (a_i) is expressed in terms of the activity coefficient (γ_i) and the concentration (C_i) [8]:

$$a_i = \gamma_i C_i \qquad \text{(Eq. 9)}$$

A calibration plot can be constructed by measuring the potentials of a series of standard solutions with known compositions, and plotting the measured potentials against the log of the analyte activity. The calibration curve is derived from the linear part of the 2-dimensional plot. The standard potential (E^o) is determined as the y-intercept of the calibration curve with slope, *S*. Once these calibration parameters (E^o and *S*) are known, one can use the potentiometric set-up as a measuring tool. In this thesis, potentiometric measurements were carried out to determine the experimental E^o from conventional calibrations.

2.7.3. Electrochemical impedance spectroscopy

Impedance is the potential/current ratio when a variable (ac) is applied to a material. It is analogous to the resistance of the system which is determined by the potential/current ratio when a constant (dc) potential is applied. In a potential-controlled electrochemical impedance spectroscopy (EIS) experiment, the system is held at a fixed potential E_{dc} and a sinusoidal excitation signal with a small amplitude $E(\omega)$ (Eq. 10), is superimposed on the (dc) potential. The resulting sinusoidal alternating current, $I(\omega)$ given by Eq. 11 is then measured.

$$E(\omega) = E\sin(\omega t) \qquad \text{(Eq. 10)}$$

$$I(\omega) = I\sin(\omega t + \varphi) \qquad \text{(Eq. 11)}$$

In Eq. 10 and Eq. 11, ω is the angular frequency that is equal to $2\pi f$, and φ is the phase shift angle between the applied signal and the resulting response. A phase shift of 0° corresponds to a pure resistor while a phase shift of 90° is a characteristic of a pure capacitor. A phase shift of 45° occurs when a Warburg impedance exists due to diffusion limitation. When the frequency of the ac wave is varied over several decades, the impedance of the system, $Z(\omega)$, is given by:

$$Z(\omega) = E(\omega)/I(\omega) \qquad \text{(Eq. 12)}$$

which can be measured as a function of the frequency [12].

The impedance $Z(\omega)$ provided by Eq. 12 is a vector quantity consisting of a real (Z') and an imaginary ($-Z''$) components:

$$Z(\omega) = (Z') - j(Z'') \qquad \text{(Eq. 13)}$$

where $j = \sqrt{-1}$ is the imaginary number. The Z' and -Z" components at each frequency can be plotted on a two-dimensional plane called "Nyquist plot" as shown below:

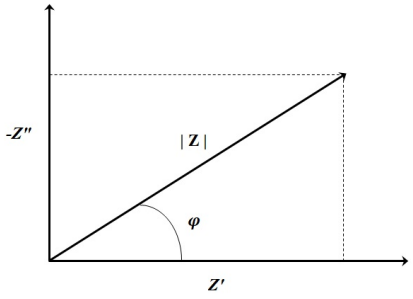

Figure 10. *Nyquist plot of the impedance (Z)*

Electrochemical impedance spectroscopy is a useful tool to study the electrochemical processes occurring in the bulk solution and at the electrode-solution interface. In this thesis, EIS was used to characterize the electrochemical behavior of conducting polymers.

2.7.4. Energy dispersive analysis of X-ray

Energy dispersive analysis of X-ray (EDAX) is an analytical technique used to obtain the elemental composition of a sample. It uses high-energy electron beam that strikes a sample surface and ejects an electron from the inner energy shell of an atom. The resulting vacancy is filled by an electron from a high energy shell. The relaxation process from a high energy to a lower energy state releases energy in the form of X-ray. The wavelength of the emitted radiation is equal to the energy difference of the electronic levels involved which is unique for every element. The amount of X-ray emitted by a particular element is related to its concentration in the sample. A typical EDAX spectrum indicates the number of counts versus the emitted X-ray energy and provides information on the relative concentrations of elements present in the sample [41]. In this thesis, EDAX was used for compositional analysis of conducting polymer films.

3. Experimental Procedure

3.1. Chemicals

3,4-ethylenedioxythiophene (EDOT > 97%) was purchased from Bayer AG. Gold(III) chloride trihydrate ($HAuCl_4 \cdot 3H_2O \geq 99.9\%$), Poly(sodium 4-styrenesulfonate) (NaPSS; MW ~ 70,000) and Potassium chloride (KCl, ≥ 99%) were obtained from Sigma-Aldrich. Poly(vinyl chloride) (PVC) of high molecular weight, Potassium ionophore I (valinomycin), potassium tetrakis(4-chlorophenyl)borate (KTpClPB), bis(2-ethylhexyl) sebacate (DOS), 2-nitrophenyl octyl ether(o-NPOE), tridodecylmethylammonium chloride (TDMACl), and tetrahydrofuran (THF, >99.5%) were Selectophore reagents from Fluka. All the other chemicals used were analytical-reagent grade. Distilled and deionized water (ELGA Purelab Ultra; resistivity 18.2 MΩcm) was used to prepare all solutions.

3.2. Electrochemical synthesis of PEDOT(PSS) and PEDOT(Cl)

3.2.1. Electrode preparation and modification

Glassy carbon (GC) electrodes (area=0.07 cm^2) were polished using abrasive paper (mesh size 280, 400, 600, 800, 1000), diamond paste (15µm, 9µm, 3µm, 1µm) and alumina slurry (0.3µm) and rinsed with water. The electrodes were then cleaned ultrasonically with ethanol (15 mins) and deionized water (15 mins).

To study the effect of the electronically conducting substrate on the electrode potential stability, gold nanoparticles-modified glassy carbon (GC-AuNPs) substrates were prepared. Preparation of GC-AuNPs electrodes was based on the procedure by Jayakumar et al. [7] with some modifications. Gold nanoparticles were deposited on polished GC electrodes from an aqueous solution of 0.01 M $HAuCl_4 \cdot 3H_2O$ and 0.1 M KCl as supporting electrolyte. The electrochemical deposition was carried out using cyclic voltammetry in the potential range of -1.5 to 2.6 V at a scan rate of 0.1 V/s for 8 cycles. The reference electrode used was Ag/AgCl/ 3 M KCl (Metrohm, 6.0733.100, Switzerland) and the auxiliary electrode was a GC rod. Figure 11 shows the growth of the AuNPs film indicated by the increase in current as the number of potential cycle increases. After 8 potential cycles, golden colored deposits were observed on the surface of the GC electrodes that could be seen with naked eyes. The GC-AuNPs electrodes were then rinsed thoroughly with deionized water.

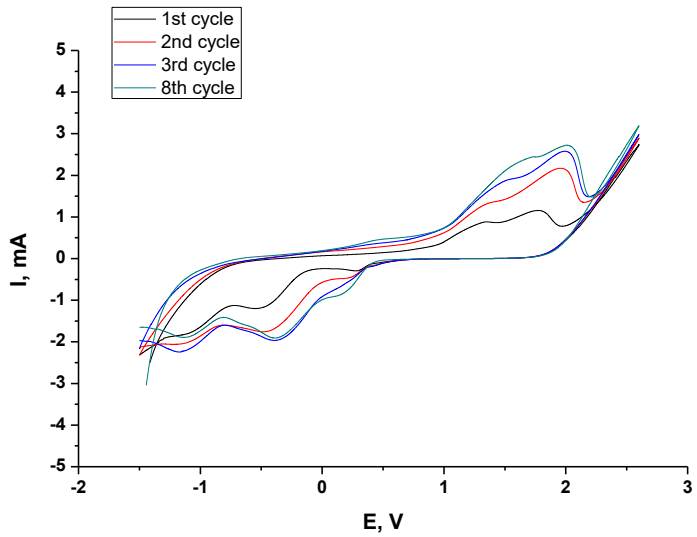

Figure 11. *Cyclic voltammograms (1st, 2nd, 3rd, and 8th cycle) of gold nanoparticle electro-deposition on glassy carbon electrode in a solution containing 10^{-2} M HAuCl4·3H_2O and 0.1 M KCl using a scan rate of 0.1 V/s.*

3.2.2. Galvanostatic polymerization of PEDOT(PSS) and PEDOT(Cl)

The electrochemical synthesis of PEDOT(PSS) and PEDOT(Cl) was based on the earlier work of Bobacka [3] and carried out using a single-compartment two-electrode electrochemical cell connected to an Autolab General Purpose Electrochemical System (AUTO30.FRA2-Autolab Eco Chemie, B.V., The Netherlands). The working electrode was a glassy carbon (GC) disk or a gold nanoparticles-modified GC (GC-AuNPs) electrode of the same area. The auxiliary electrode was a GC rod. No reference electrode was used to avoid contamination. Galvanostatic polymerization of PEDOT(PSS) was done using a deaerated solution of 0.01 M EDOT and 0.1 M poly(sodium 4-styrenesulfonate) (NaPSS) as supporting electrolyte while for PEDOT(Cl), the solution used was 0.01 M EDOT + 0.1 M KCl. A constant current of 0.014 mA (0.2 mA/cm^2) was applied on the working electrodes for 714 s to produce a polymerization charge of about 10 mC. After polymerization, the electrodes (GC/PEDOT(PSS), GC-AuNPs/PEDOT(PSS), GC/PEDOT(Cl) and GC-AuNPs/PEDOT(Cl)) were conditioned in 0.01 M KCl or 0.01 M $AgNO_3$ for at least two days before further characterization and calibration.

3.3. Fabrication of solid-contact K^+-ISEs

Solid-contact K^+-ISEs were prepared by applying an ion-selective membrane (ISM) cocktail on the GC/PEDOT(PSS), GC-AuNPs/PEDOT(PSS), GC/PEDOT(Cl), and GC-AuNPs/PEDOT(Cl) electrodes by drop casting. Three replicates were prepared for each electrode type. The dry fraction of the ISM cocktail has the following composition in % (w/w): 1.2% valinomycin, 0.4% KTpClPB, 66.4% DOS, and 32.0% PVC with a total mass of 0.7968 g. These components were dissolved in 3.0 mL THF (dry fraction of the membrane cocktail is ca 23% w/w). 100 µL of the ISM cocktail was applied on the surface of each electrode. After drying of the membrane, the GC/PEDOT(PSS)/K^+-ISM, GC-AuNPs/PEDOT(PSS)/K^+-ISM, GC/PEDOT(Cl)/K^+-ISM and GC-AuNPs/PEDOT(Cl)/K^+-ISM electrodes were conditioned in 0.01 M KCl for at least two days before further measurements.

3.4. Fabrication of solid-contact Cl^--ISEs

Three types of solid-contact chloride ion-selective electrodes were prepared: GC/PEDOT(Cl)/Cl^--ISM, GC-AuNPs/PEDOT(Cl)/Cl^--ISM, and Ag/AgCl/Cl^--ISM. The GC/PEDOT(Cl)/Cl^--ISM and GC-AuNPs/PEDOT(Cl)/Cl^--ISM were prepared by applying 100 µL of the Cl^--ISM cocktail on the GC/PEDOT(Cl) or GC-AuNPs/PEDOT(Cl) electrodes which were

prepared as in 3.2.2. Three replicates were prepared for both types of electrodes. The chloride ion-selective membrane (ISM) cocktail has the following composition in % (w/w): 34% PVC, 51% o-NPOE, and 15% TDMACl and a total weight of 0.7524 g. These components were dissolved in 3.0 mL THF (the dry fraction of the membrane cocktail is ca 22% (w/w)).

The Ag/AgCl/Cl^--ISM electrodes were prepared by applying 100 µL of the Cl^--ISM cocktail on Ag/AgCl electrodes. An Ag/AgCl electrode was prepared by passing a current of 0.1 mA through a silver disk electrode immersed in 1 M KCl for two hours using a galvanostat (coulometer type E211, Switzerland). Three replicates were prepared. Prior to galvanostatic deposition, the silver disk electrodes were polished using abrasive paper (mesh size 280, 400, 600, 800, 1000), diamond paste (15µm, 9µm, 3µm, 1µm) and alumina (0.3µm). The electrodes were then rinsed with water and ethanol and cleaned ultrasonically.

After drying of the membrane, the GC/PEDOT(Cl)/Cl^--ISM, GC-AuNPs/PEDOT(Cl)/Cl^--ISM and Ag/AgCl/Cl^--ISM electrodes were conditioned in 0.01 M KCl for at least two days before further measurements.

3.5. Cyclic Voltammetry (CV) Measurements

Cyclic voltammograms were recorded using a conventional one-compartment three electrode electrochemical cell connected to the Autolab General Purpose Electrochemical System. The studied electrode was connected as the working electrode. The reference electrode was a single-junction Ag/AgCl/3M KCl (Metrohm, 6.0733.100, Switzerland) and the auxiliary electrode was a GC rod. The studied electrodes were GC/PEDOT(PSS) and GC/PEDOT(Cl). Cyclic voltammograms were recorded for five cycles in the potential range -0.5V to 0.5V with a scan rate of 0.1 V/s in 0.1 M KCl solution or 0.1 M KNO_3 solution. The KCl or KNO_3 solutions were first deaerated with N_2 for 15 minutes, and then the N_2 gas outlet was kept above the solution during the measurement.

3.6. Electrochemical impedance spectroscopy (EIS)

Electrochemical impedance spectroscopy (EIS) measurements were done in a deaerated solution of 0.1 M KCl using the Autolab Frequency Response Analyzer System (AUTO30.FRA2-Autolab Eco Chemie, B.V., The Netherlands) connected to a conventional one-compartment three-electrode electrochemical cell. The reference electrode was Ag/AgCl/3M KCl (Metrohm) and the auxiliary electrode was a GC rod. For the impedance measurements, a sinusoidal

excitation signal with an excitation amplitude of 10 mV was used in the frequency range of 100 kHz-10 mHz. The impedance spectra were recorded at the open-circuit potential of GC/PEDOT(PSS), GC/PEDOT(Cl), GC-AuNPs/PEDOT(PSS) and GC-AuNPs/PEDOT(Cl) electrodes before and after applying the ISM on each electrode.

3.7. Chronopotentiometry

After applying the ISM and at least one day of conditioning, chronopotentiometric measurements were carried out on GC/PEDOT(PSS)/K^+-ISM, GC/PEDOT(Cl)/K^+-ISM, GC-AuNPs/PEDOT(PSS)/K^+-ISM, GC-AuNPs/PEDOT(Cl)/K^+-ISM, GC/PEDOT(Cl)/Cl^--ISM, and GC-AuNPs/PEDOT(Cl)/Cl^--ISM electrodes. The same Autolab instrument was used as in cyclic voltammetry measurements. The measurements were done by applying a constant current of +1 nA for 60 s followed by -1 nA for another 60 s and measuring the potential of the electrodes as a function of time. The measurements were performed at room temperature (23 ± 2 ^oC).

3.8. Potentiometric measurements

Potentiometric measurements were done using a 16-channel millivoltmeter (Lawson Labs. Inc., Malvern, PA, USA). The reference electrode used was a double-junction Ag/AgCl/3M KCl (Metrohm, 6.0726.100, Switzerland) with a salt bridge containing 1 M LiOAc. Automatic calibration was performed using two Metrohm Dosino 800 instruments equipped with burets of 50 mL capacity (Herisau, Switzerland). The activity coefficients were calculated according to the extended Debye-Hückel equation [42]. All calibrations were done at room temperature (23±2^oC).

3.9. Scanning electron microscopy (SEM)/ energy dispersive analysis of X-ray (EDAX)

SEM/EDAX measurements were done to study the morphology and elemental analysis of PEDOT(PSS) films. The instrument used was a LEO Gemini 1530 (Oberkochen, Germany) scanning electron microscope equipped with a Thermo Scientific UltraDry Silicon Drift Detector (SDD) (Thermo Scientific Inc., Madison, Wisconsin, U.S.A). In the EDAX, a sample area of 3.5~6.4 mm^2 was taken for analysis. For SEM/EDAX measurements, PEDOT(PSS) was deposited on platinum electrodes (0.10 - 0.15 cm^2) using the galvanostatic polymerization method in a deaerated solution of 0.01 M EDOT and 0.1 M poly(sodium 4-styrenesulfonate) (NaPSS) as supporting electrolyte. The current was chosen to obtain a polymerization charge of 10 mC. One of the prepared Pt/PEDOT(PSS) electrodes was kept unconditioned, two

Pt/PEDOT(PSS) electrodes were conditioned in 0.01 M KCl and three sets (two electrodes each) of Pt/PEDOT(PSS) electrodes were conditioned in 0.01 M $AgNO_3$. Prior to SEM/EDAX measurements, cyclic voltammograms for one set of Pt/PEDOT(PSS) electrodes (conditioned in 0.01 M $AgNO_3$) were recorded in 0.1 M KCl and for one set, cyclic voltammograms were recorded in 0.1 M KNO_3. No cyclic voltammograms were recorded for the third set of Pt/PEDOT(PSS) electrodes conditioned in 0.01 M $AgNO_3$ or for the Pt/PEDOT(PSS) electrodes conditioned in 0.01 M KCl. For all the performed cyclic voltammetry measurements, the procedure described in section 3.5 was used.

4. Results and discussion

4.1. Characterization of solid-contact K^+-ISEs and evaluation of E^o stability

4.1.1. Cyclic voltammetry (CV) measurements

The redox capacitance of PEDOT(PSS) and PEDOT(Cl) solid-contacts was studied by recording the cyclic voltammograms of GC/PEDOT(PSS) and GC/PEDOT(Cl) electrodes in 0.1 M KCl at the potential range of -0.5 to 0.5 V with the scan rate of 0.1 V/s. The obtained cyclic voltammograms for GC/PEDOT(PSS) and GC/PEDOT(Cl) were compared to that of bare GC electrode measured under the same conditions. Typical cyclic voltammograms of GC/PEDOT(PSS), GC/PEDOT(Cl), and bare GC electrodes are shown in Figure 12.

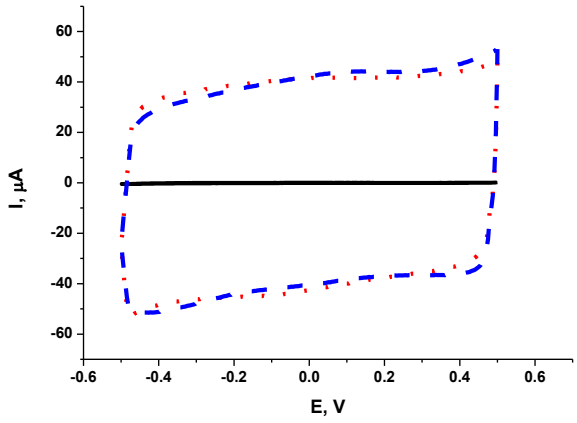

Figure 12. *Cyclic voltammograms (5th cycle) of bare GC (solid line), GC/PEDOT(PSS) (dotted line) and GC/PEDOT(Cl) (dashed line) recorded in 0.1 M KCl at a scan rate of 0.1 V/s.*

In the potential range of -0.5 to 0.5 V, the capacitive current of GC/PEDOT(Cl) and GC/PEDOT(PSS) are almost identical while for the bare GC electrode, a negligible current was observed. A high capacitive current indicates a high redox capacitance which is one of the stability conditions required for solid-state ion-selective electrodes [3]. The redox capacitance can also be estimated from impedance measurements at low frequencies as will be discussed in section 4.1.3.

4.1.2. Potentiometric measurements

The prepared GC/PEDOT(PSS), GC-AuNPs/PEDOT(PSS), GC/PEDOT(Cl), and GC-AuNPs/PEDOT(Cl) electrodes were subjected to potentiometric measurements using 10^{-1} - 10^{-6} M KCl solutions. The reference electrode used was Ag/AgCl/3M KCl (Metrohm) with a salt bridge containing 1M LiOAc. Prior to calibrations, the GC/PEDOT(PSS), GC-AuNPs/PEDOT(PSS), GC/PEDOT(Cl), and GC-AuNPs/PEDOT(Cl) electrodes were conditioned in 0.01 M KCl for at least one day; and were conditioned in the same solution in between calibrations. Calibration plots for GC/PEDOT(PSS), GC-AuNPs/PEDOT(PSS), GC/PEDOT(Cl), and GC-AuNPs/PEDOT(Cl) electrodes are shown in Figure 13. The error bars in the calibration curves indicate the standard deviation of the measured potentials for the same electrodes during certain days of measurement (see Table 1). The obtained calibration data are summarized in Table 1.

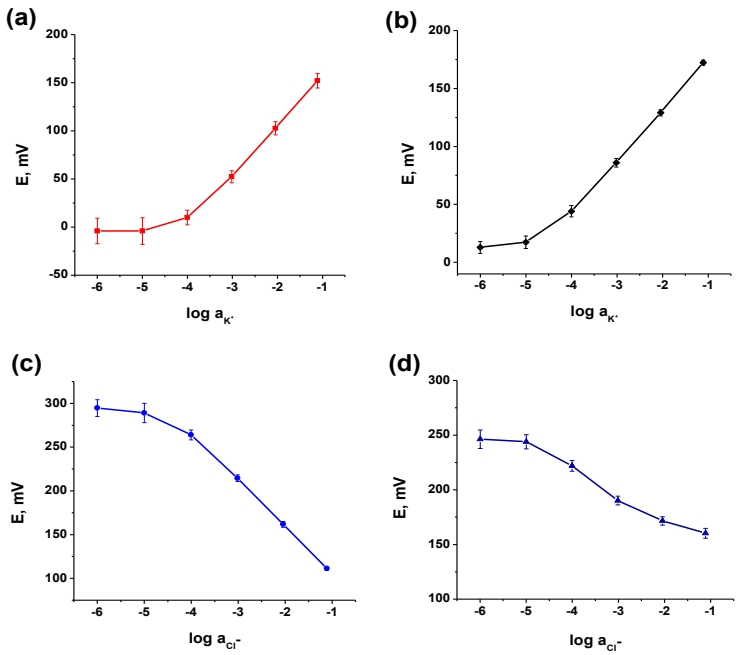

Figure 13. *Calibration plots for GC/PEDOT(PSS) (a), GC-AuNPs/PEDOT(PSS) (b), GC/PEDOT(Cl) (c) and GC-AuNPs/PEDOT(Cl) electrodes (d) in 10^{-1}-10^{-6} M KCl solutions. The error bars on the calibration curves correspond to the standard deviations of the measured potentials for the same electrodes during different days of repeated calibrations (see Table 1).*

As can be observed in Figure 13a and Figure 13b, the potentiometric responses of GC/PEDOT(PSS) and GC-AuNPs/PEDOT(PSS) electrodes were cationic. This is due to the negative sites provided by the immobile polystyrenesulfonate (PSS^-) doping anions which are then compensated by potassium ions [3]. On the other hand, the potentiometric responses of GC/PEDOT(Cl) (Figure 13c) and GC-AuNPs/PEDOT(Cl) (Figure 13d) were anionic as the positive charge of the oxidized PEDOT film is compensated by mobile chloride ions. The potentiometric response for the GC-AuNPs/PEDOT(Cl) electrode however, was not as linear as that for GC/PEDOT(Cl) in the same range of Cl^- ion activity. One possible reason for this is the presence of residual tetrachloroaurate(III) ($AuCl4^-$) in the GC-AuNPs/PEDOT(Cl) electrode, resulting from the AuNPs deposition step. In this case, the GC-AuNPs/PEDOT(Cl) electrode could give a mixed response for both K^+ and Cl^- ions. However, further experiments must be carried out to prove this assumption.

Table 1. *Calibration data for GC/PEDOT(PSS), GC-AuNPs/PEDOT(PSS), GC/PEDOT(Cl) and GC-AuNPs/PEDOT(Cl) electrodes. The standard deviation indicates the variations in the calibration parameters obtained for the same electrode during different days of calibration.*

Electrode	Standard potential (E^o) ± SD (mV)	Slope ± SD (mV/decade)	Linear Range (M)
GC/PEDOT(PSS) *	205.1 ± 7.9	49.4 ± 1.2	10^{-1}-10^{-4} (K^+)
GC-AuNPs/PEDOT(PSS)**	235.7 ± 3.6	48.4 ± 0.4	10^{-1}-10^{-4} (K^+)
GC/PEDOT(Cl)*	53.3 ± 0.5	-53.0 ± 1.2	10^{-1}-10^{-4} (Cl^-)
GC-AuNPs/PEDOT(Cl)***	--	--	--

* calibrations done on the 2nd, 5th, 6th and 8th days of conditioning in 0.01 M KCl
** calibrations done on the 2nd, 4th and 7th days of conditioning in 0.01 M KCl
*** non-linear potentiometric response

As shown in Table 1, the linear responses of GC/PEDOT(PSS) and GC-AuNPs/PEDOT(PSS) electrodes were in the activity range of 10^{-1}-10^{-4} M of K^+. On the other hand, the linear response of GC/PEDOT(Cl) was in the activity range of 10^{-1}-10^{-4} M of Cl^-. The slope of the calibration curve for GC/PEDOT(PSS) was 49.4 ± 1.2 mV/decade while the slope of the GC-AuNPs/PEDOT(PSS) electrode was 48.4 ± 0.4 mV/decade. However, the standard deviation of the E^o was smaller for GC-AuNPs/PEDOT(PSS) (± 3.6 mV) than that of GC/PEDOT(PSS) (± 7.9 mV). The slope of the calibration curve for the GC/PEDOT(Cl) electrode was -53.0 ± 1.2 mV/decade and the standard deviation of E^o was ± 0.5 mV, which is lower than either GC/PEDOT(PSS) or GC-AuNPs/PEDOT(PSS) electrodes.

4.1.3. Electrochemical Impedance Spectroscopy (EIS)

In this experiment, electrochemical impedance spectroscopy was used to study the electrochemical processes involving the PEDOT solid-contact occurring in the bulk solution and at the electrode-solution interface. EIS measurements for GC/PEDOT(PSS), GC-AuNPs/PEDOT(PSS), GC/PEDOT(Cl), and GC-AuNPs/PEDOT(Cl) electrodes, with and without ISM, were carried out in 0.1 M KCl in the frequency range of 100 kHz-10 mHz. Typical impedance spectra of GC/PEDOT(PSS), GC-AuNPs/PEDOT(PSS), GC/PEDOT(Cl), and GC-AuNPs/PEDOT(Cl) electrodes are shown in Figure 14.

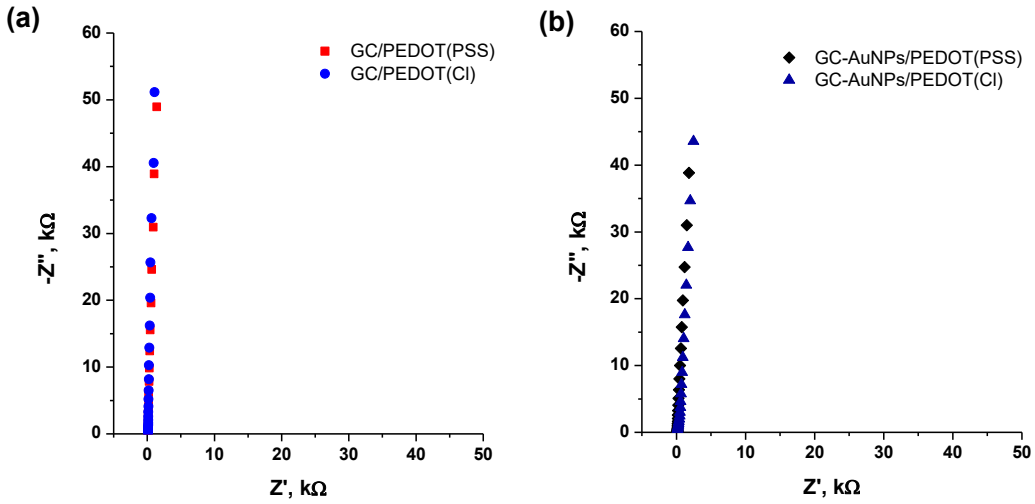

Figure 14. *Impedance spectra of GC/PEDOT(PSS), GC/PEDOT(Cl) (a), GC-AuNPs/PEDOT(PSS), and GC-AuNPs/PEDOT(Cl) (b) recorded in 0.1 M KCl at* ΔE_{ac} *= 10 mV. The frequency range was 100 KHz-10 mHz.*

The shape of the impedance spectra for both GC/PEDOT(PSS) and GC/PEDOT(Cl) electrodes (Figure 14a) at low frequencies closely resemble that of an ideal capacitor which indicates that all the redox sites of the polymer films are involved in the doping process [3]. This behavior is typical for PEDOT films in aqueous electrolyte [21]. At the low-frequency region, the imaginary part of impedance (*-Z"*) is related to the low-frequency capacitance (C_{LF}) by the following equation:

$$C_{LF} = 1/[2\pi f(-Z'')] \qquad \text{(Eq. 14)}$$

Where f is the lowest frequency used to record the spectra (0.01 Hz). Using Eq. 14, the calculated C_{LF} was 325 for GC/PEDOT(PSS) and 311 µF for GC/PEDOT(Cl). These results were in good agreement with those obtained in the cyclic voltammetry measurements which showed that GC/PEDOT(Cl) and GC/PEDOT(PSS) electrodes have almost identical redox capacitance. On the other hand, the impedance spectra for both GC-AuNPs/PEDOT(PSS) and GC-AuNPs/PEDOT(Cl) electrodes (Figure 14b) also resemble that of an ideal capacitor. However, the C_{LF} for GC-AuNPs/PEDOT(PSS) was higher (410 µF) than that of GC-AuNPs/PEDOT(Cl) (365 µF). The C_{LF} for GC-AuNPs/PEDOT(PSS) (410 µF) was also higher than that of GC/PEDOT(PSS) (325 µF) or GC/PEDOT(Cl) (311 µF).

After applying the K^+-selective membrane, the impedance spectra of the GC/PEDOT(PSS)/K^+-ISM, GC-AuNPs/PEDOT(PSS)/K^+-ISM, GC/PEDOT(Cl)/K^+-ISM, and GC-AuNPs/PEDOT(Cl)/K^+-ISM electrodes were recorded in 0.1 M KCl at 100 kHz-10 mHz (Figure 15).

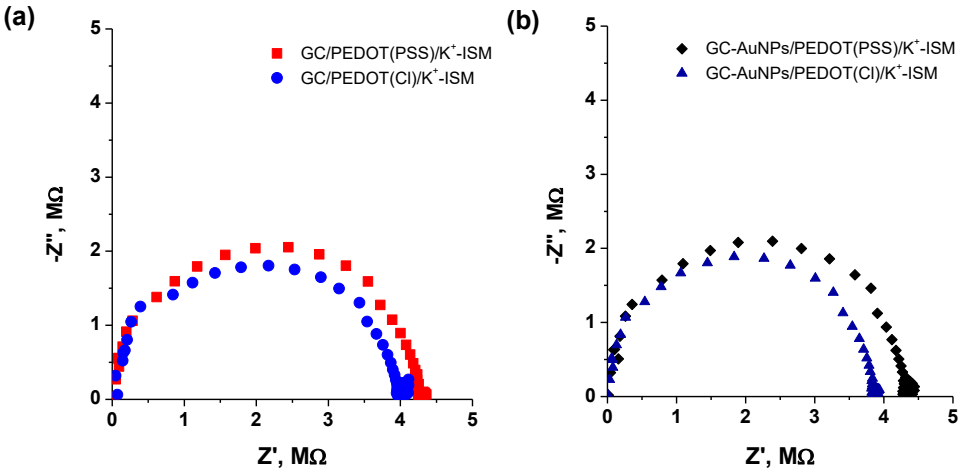

Figure 15. *Impedance spectra of GC/PEDOT(PSS)/K^+-ISM, GC/PEDOT(Cl)/K^+-ISM (a) GC-AuNPs/PEDOT(PSS)/K^+ISM, and GC-AuNPs/PEDOT(Cl)/ K^+-ISM (b) recorded in 0.1 M KCl at ΔE_{ac} = 10 mV. The frequency range was 100 KHz-10 mHz.*

The high-frequency semicircle observed in the impedance spectra of GC/PEDOT(PSS)/K^+-ISM, GC/PEDOT(Cl)/K^+-ISM, GC-AuNPs/PEDOT(PSS)/K^+-ISM, and GC-AuNPs/PEDOT(Cl)/K^+-ISM electrodes in Figure 15 is characteristic of the PVC-based ion-selective membrane and is independent of the solid-contact used [3]. The applied ion-selective membrane in GC/PEDOT(PSS)/K^+-ISM, GC/PEDOT(Cl)/K^+-ISM, GC-AuNPs/PEDOT(PSS)/K^+-ISM, and GC-AuNPs/PEDOT(Cl)/K^+-ISM electrodes are supposed to have the same thicknesses because similar volumes of ISM cocktail were applied. The absence of a low-frequency semicircle branch in the impedance spectrum of all the K^+-ISEs indicates a good ion-to-electron transduction resulting from high capacitance (C_{LF}) of the polymer films at low frequencies [3].

4.1.4. Chronopotentiometry

The potential stability of the fabricated solid-contact ISEs was studied using the constant-current chronopotentiometric method suggested by Bobacka [3]. A current of ±1 nA was applied to the working electrodes in 0.1 M KCl and the resulting potentials were recorded. Chronopotentiograms of the GC/PEDOT(PSS)/K^+-ISM, GC/PEDOT(Cl)/K^+-ISM, GC-AuNPs/PEDOT(PSS)/K^+-ISM, and GC-AuNPs/PEDOT(Cl)/K^+-ISM electrodes are shown in Figure 16.

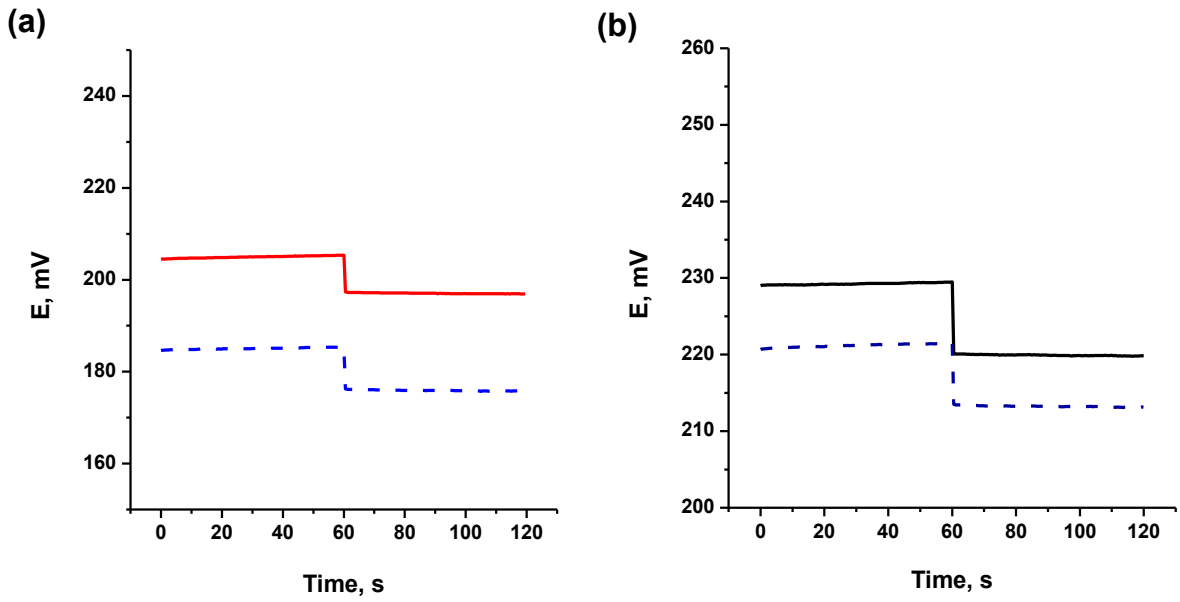

Figure 16. *Chronopotentiograms of GC/PEDOT(PSS)/K⁺-ISM (solid red line), GC/PEDOT(Cl)/K⁺-ISM (dashed blue line) (a), GC-AuNPs/PEDOT(PSS)/K⁺-ISM (solid black line) and GC-AuNPs/PEDOT(Cl)/K⁺-ISM (dashed blue line) (b) recorded in 0.1 M KCl. Applied current is +1 nA for 60 s and -1 nA for 60s.*

The chronopotentiograms of all the electrodes showed a potential jump as the applied current changed from +1 nA to -1 nA (Figure 16). This potential jump can be used to estimate the total resistance (R_T) of the electrodes using the following formula:

$$R_T = E/i \qquad \text{(Eq. 15)}$$

Where *E* represents the potential change due to the applied current *i*. The calculated total resistance for GC/PEDOT(PSS)/K⁺-ISM was 4.8 MΩ while that for GC/PEDOT(Cl)/K⁺-ISM was 4.3 MΩ. On the other hand, the calculated total resistance for GC-AuNPs/PEDOT(PSS)/K⁺-ISM was 4.7 MΩ while that for GC-AuNPs/PEDOT(Cl)/K⁺-ISM was 4.0 MΩ. These values are in good agreement with the bulk resistance estimated from impedance measurements (see Figure 15).

The potential drift of the fabricated ISEs was determined from the slopes ($\Delta E/\Delta t$) of the E-t curves at longer times. The potential drift of solid-contact ISEs is related to the low-frequency capacitance (C_{LF}) by the following equation:

$$Potential\ drift\ (\Delta E/\Delta t) = \ i/C_{LF} \qquad \text{(Eq. 16)}$$

From this formula, the low-frequency capacitance C_{LF} of GC/PEDOT(PSS)/K^+-ISM, GC/PEDOT(Cl)/K^+-ISM, GC-AuNPs/PEDOT(PSS)/K^+-ISM, and GC-AuNPs/PEDOT(Cl)/K^+-ISM electrodes were calculated and are shown in Table 2.

Table 2. *Results from chronopotentiometric measurements carried out on the solid-contact potassium ion-selective electrodes.*

Electrode	$\Delta E/\Delta t$ (μV/s)	C_{LF} (μF)
GC/PEDOT(PSS)/K^+-ISM	7.7	130
GC-AuNPs/PEDOT(PSS)/K^+-ISM	5.5	182
GC/PEDOT(Cl)/K^+-ISM	10.4	96
GC-AuNPs /PEDOT(Cl)/K^+-ISM	8.3	120

Due to applying PVC-based K^+-ISM, the C_{LF} values obtained using chronopotentiometry are lower than those determined for GC/PEDOT(PSS), GC/PEDOT(Cl), GC-AuNPs/PEDOT(PSS), and GC-AuNPs/PEDOT(Cl) electrodes using EIS in KCl solution. This means that the ion-transport to/from the polymer film depends on the contacting medium and it is more efficient in an electrolyte medium than in a PVC membrane.

4.1.5. Evaluation of E^o stability

The solid-contact K^+-ISEs (GC/PEDOT(PSS)/K^+-ISM, GC/PEDOT(Cl)/K^+-ISM, GC-AuNPs/PEDOT(PSS)/K^+-ISM, and GC-AuNPs/PEDOT(Cl)/K^+-ISM) were prepared as described in Section 3.3. After conditioning in 0.01 M KCl for at least two days, the electrodes were calibrated in 10^{-1} to 10^{-7} M KCl solutions. The reference electrode was Ag/AgCl/3M KCl (Metrohm) with a salt bridge containing 1M LiOAc. The standard potential (E^o) was determined as the y-intercept of the linear part of the calibration curve. The calibrations were repeated for several weeks and the electrodes were kept conditioned in 0.01 M KCl in between calibrations. The stability of E^o was evaluated as the standard deviation of the experimental E^o values obtained from all the calibrations carried out for each electrode.

Figure 17 shows the calibration curves for each type of electrode obtained at certain days of conditioning. The calibration curves for GC/PEDOT(PSS)/K^+-ISM (Figure 17a) and GC/PEDOT(Cl)/K^+-ISM (Figure 17b) were shifted to more positive potentials at longer periods of conditioning, with GC/PEDOT(Cl)/K^+-ISM having smaller changes in the measured

potentials. The calibration curves for GC-AuNPs/PEDOT(PSS)/K^+-ISM (Figure 17c) and GC-AuNPs/PEDOT(Cl)/K^+-ISM (Figure 17d) were shifted to more positive potentials at longer periods of conditioning with comparable changes in the measured potentials.

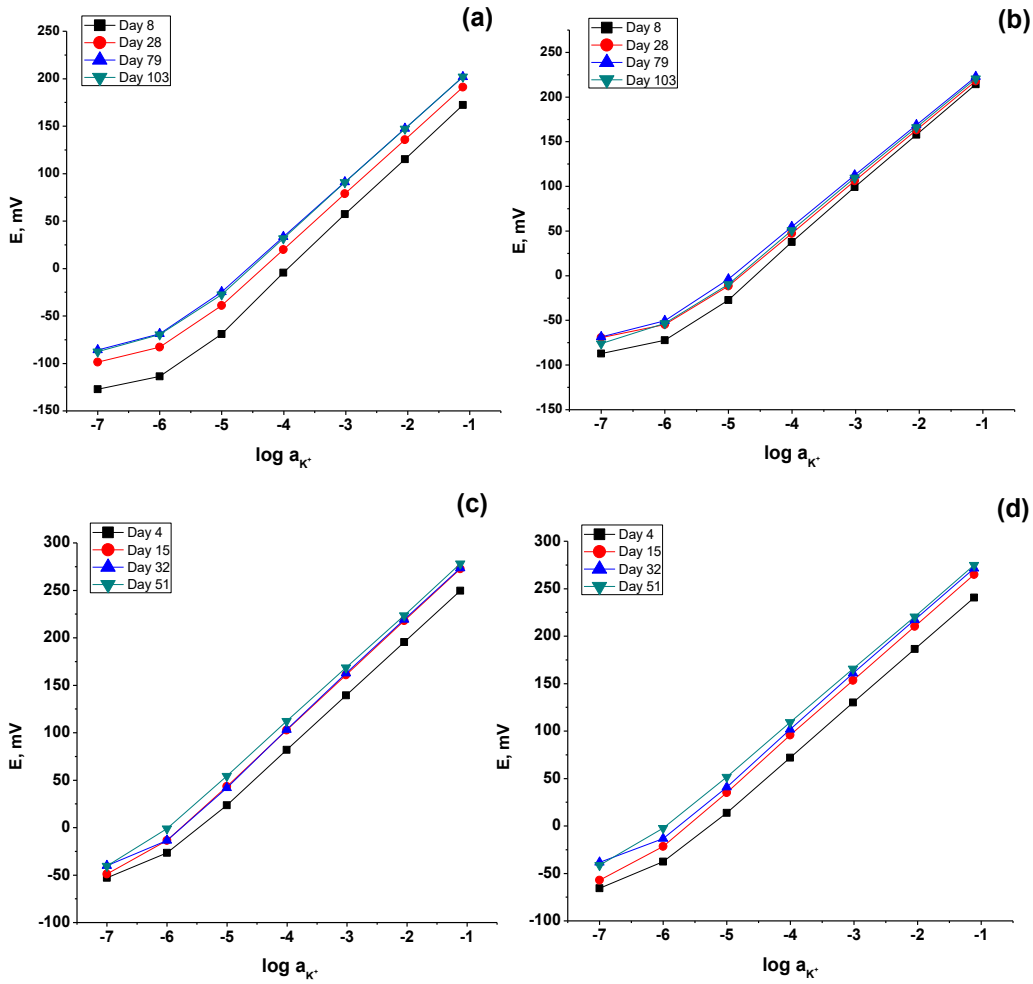

Figure 17. *Calibration plots for the GC/PEDOT(PSS)/K^+-ISM (a), GC/PEDOT(Cl)/K^+-ISM (b), GC-AuNPs/PEDOT(PSS)/K^+-ISM (c), GC-AuNPs/PEDOT(Cl)/K^+-ISM (d) electrodes at various days of conditioning. Calibration plots for respective days are indicated on each figure.*

The changes in E^o values for each type of electrode for respective conditioning periods are illustrated in Figure 18. It can be observed that for all the solid-contact K^+-ISEs studied, there was a shift towards more positive standard potentials (E^o) during the initial conditioning period which tended to stabilize at later periods of conditioning (Figure 18). In an earlier study by Mousavi et al. [34], a K^+-ISE with PEDOT doped with carbon nanotubes (CNTs) as solid contact and screen-printed carbon electrodes (SPCE) modified with multi-walled CNTs as conducting substrate, showed changes in E^o of 3 mV and 13 mV after conditioning in 0.01 M

KCl for 2 and 10 weeks, respectively. Vázquez et al. [36] reported that the potential stability of solid-state K^+-ISEs with solution-cast films of PEDOT(PSS) (Baytron P) improved when a ruthenium redox couple ($Ru(NH_3)_6^{2+3+}$) was used for cross-linking PEDOT(PSS) compared to electroinactive cations (Ca^{2+}, Mg^{2+}). The K^+-ISE electrodes treated with $Ru(NH_3)_6^{2+3+}$ showed a change in E^o of ~15 mV after 14 days of conditioning in 0.1 M KCl. In the present experiment, the highest E^o stability was observed for the GC-AuNPs/PEDOT(PSS)/K^+-ISM electrode with a maximum change in E^o of 4.9 mV during an extended conditioning period of 51 days (excluding the initial equilibration period of 10 days).

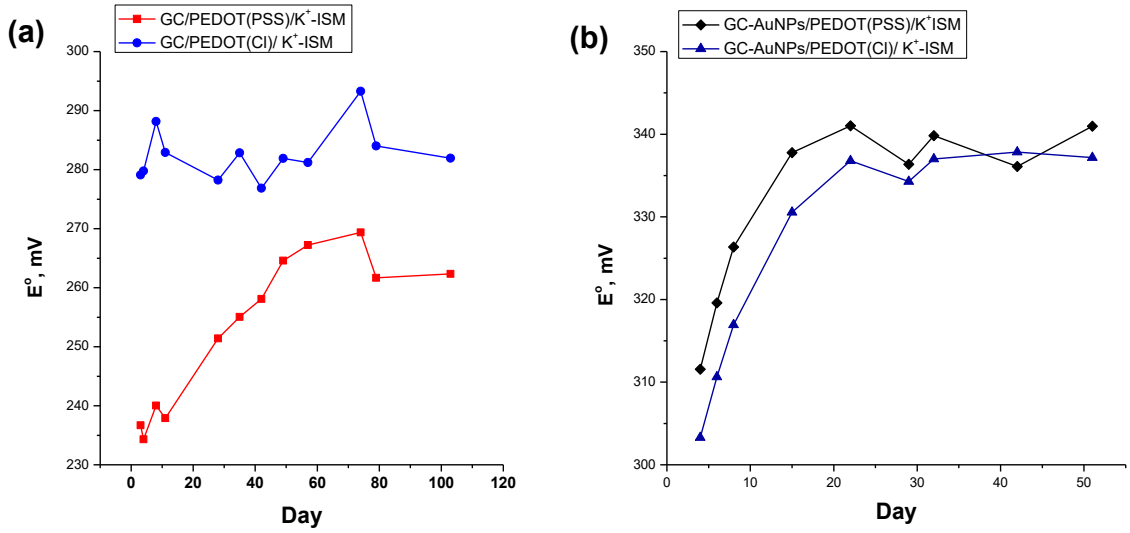

Figure 18. *Plots of standard potentials (E^o) for the GC/PEDOT(PSS)/K^+-ISM, GC/PEDOT(Cl)/K^+-ISM (a), GC-AuNPs/PEDOT(PSS)/K^+-ISM and GC-AuNPs/PEDOT(Cl)/K^+-ISM (b) at different days of calibration in KCl solutions. For the E^o stability evaluation, the E^o values after 10 days of conditioning were used.*

In this experiment, it was observed that the E^o started to stabilize after a certain period of conditioning, which varies from one type of solid-contact K^+-ISE to another. During conditioning, the ISM becomes hydrated and the ion-exchange between the ISM and the conditioning solution reaches a steady state or equilibrium [40]. In order to effectively compare the E^o stability for all the solid-contact K^+-ISEs studied, the calibration data after 10 days of conditioning were used. All the other calibration parameters measured after 10 days of conditioning were compared.

The cumulative calibration curves obtained for the GC/PEDOT(PSS)/K^+-ISM, GC/PEDOT(Cl)/K^+-ISM, GC-AuNPs/PEDOT(PSS)/K^+-ISM, and GC-AuNPs/PEDOT(Cl)/K^+-ISM electrodes after 10

days of conditioning are illustrated in Figure 19. As can be seen from Figure 19a and Figure 19b, the linear part of the calibration curves of all electrodes were in the activity range of 10^{-1}-10^{-6} M of the K^+ ion. The standard deviations of the potentials from the mean value (indicated by error bars) was higher for GC/PEDOT(PSS)/K^+-ISM than GC/PEDOT(Cl)/K^+-ISM. On the other hand the standard deviations of the measured potentials were comparable between the GC-AuNPs/PEDOT(PSS)/K^+-ISM and GC-AuNPs/PEDOT(Cl)/K^+-ISM electrodes.

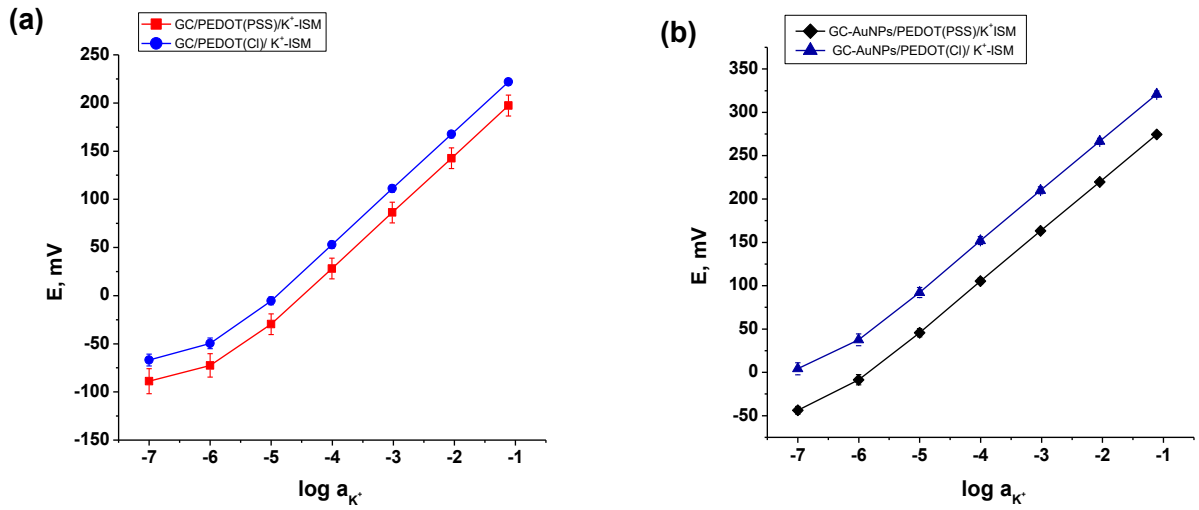

***Figure 19**. Calibration curves for the GC/PEDOT(PSS)/K^+-ISM, GC/PEDOT(Cl)/K^+-ISM (a), GC-AuNPs/PEDOT(PSS)/K^+-ISM, and GC-AuNPs/PEDOT(Cl)/K^+-ISM electrodes (b) obtained from calibration data after 10 days of conditioning. In (b) the potential values for the GC-AuNPs/PEDOT(Cl)/K^+-ISM electrode was shifted by +50 mV for better visualization. The error bars on the calibration curves correspond to the standard deviations of the measured potentials for the same electrodes during the several weeks of calibration.*

Table 3 summarizes the calibration data of the GC/PEDOT(PSS)/K^+-ISM, GC/PEDOT(Cl)/K^+-ISM, GC-AuNPs/PEDOT(PSS)/K^+-ISM, and GC-AuNPs/PEDOT(Cl)/K^+-ISM electrodes taken after 10 days of conditioning. The parameter values reflected in Table 3 correspond to the electrodes with the lowest E^o standard deviations among three identical electrodes prepared for each electrode type. The calibration data for all the solid-contact K^+-ISEs prepared for this experiment can be found in the appendix of this thesis. The performance of a commercial potassium ISE (Thermo Scientific Orion) is also included in Table 3 for comparison. As observed, the standard deviation of E^o for GC/PEDOT(PSS)/K^+-ISM (± 9.6 mV) is higher than that for GC/PEDOT(Cl)/K^+-ISM (± 4.6 mV). The slopes for GC/PEDOT(PSS)/K^+-ISM and

GC/PEDOT(Cl)/K^+-ISM electrodes were almost identical (~ 56 mV/decade) in the same linear activity range (10^{-1}-10^{-6} M of K^+). On the other hand, the standard deviation of E^o for GC-AuNPs/PEDOT(PSS)/K^+-ISM (± 2.2 mV) is comparable to that for GC-AuNPs/PEDOT(Cl)/K^+-ISM (± 2.8 mV). The slopes for GC-AuNPs/PEDOT(PSS)/K^+-ISM and GC-AuNPs/PEDOT(Cl)/K^+-ISM electrodes were almost identical (~ 58 mV/decade) in the same linear activity range (10^{-1}-10^{-6} M of K^+).

Table 3. *Calibration data for the fabricated solid-contact K^+-ISEs and a commercial K^+-ISE obtained after 10 days of conditioning in 0.01 M KCl. The standard deviation indicates the variations in the calibration parameters obtained for the same electrode during different days of calibration. The overall time frame of the stability study is indicated by the conditioning period for each type of electrode.*

Electrode	Conditioning time (day)	Standard potential (E^o) ± SD (mV)	Slope ± SD (mV/decade)	Linear Range (M)
GC/PEDOT(PSS)/K^+-ISM	103	258.6 ± 9.6	56.3 ± 0.6	10^{-1}-10^{-6}
GC/PEDOT(Cl)/K^+-ISM	103	282.6 ± 4.6	56.6 ± 0.6	10^{-1}-10^{-6}
GC-AuNPs/PEDOT(PSS)/K^+-ISM	51	338.7 ± 2.2	58.2 ± 1.0	10^{-1}-10^{-6}
GC-AuNPs/PEDOT(Cl)/K^+-ISM	51	335.6 ± 2.8	58.3 ± 0.8	10^{-1}-10^{-6}
Commercial K^+-ISE*	--	89.5 ± 3.8	57.0 ± 1.0	10^{-1}-10^{-5}

* no conditioning required in-between calibrations

Results from this experiment show that for the K^+-ISEs with glassy carbon (GC) as conducting substrate, the PEDOT(Cl) solid-contact gave better E^o stability than when PEDOT(PSS) was used as solid-contact. This was evident despite comparable redox capacitance of PEDOT(PSS) and PEDOT(Cl) films obtained from cyclic voltammetry and impedance measurements (see Figure 12 and Figure 14a). On the other hand, when gold nanoparticles-modified glassy carbon (GC-AuNPs) was used as conducting substrate, the E^o stability of the K^+-ISE with PEDOT(PSS) as solid-contact was comparable to that with PEDOT(Cl) as solid-contact. Consequently, the E^o stability is better when GC-AuNPs was used as conducting substrate than when glassy carbon was used as conducting substrate. This suggests that the conducting substrate or solid-contact has an effect on the ion-to-electron transduction processes in the studied solid-contact K^+-ISEs.

4.2. Electrochemical properties of GC/PEDOT(PSS) conditioned in 0.01 M $AgNO_3$

GC/PEDOT(PSS) electrodes were prepared as in 3.2.2 and conditioned in 0.01 M $AgNO_3$. The conditioned GC/PEDOT(PSS) electrodes were then characterized using cyclic voltammetry and potentiometry. To study the accumulation of silver on the PEDOT(PSS) film after conditioning, scanning electron microscopy (SEM) and energy dispersive analysis of X-ray (EDAX) were carried out on Platinum (Pt)/PEDOT(PSS) electrodes conditioned in 0.01 M $AgNO_3$ in the same manner as the GC/PEDOT(PSS) electrodes.

4.2.1. Cyclic voltammetry measurements

Cyclic voltammograms for GC/PEDOT(PSS) electrodes were recorded in 0.1 M KNO_3 or 0.1 M KCl at a scan rate of 0.1 V/s after four days of conditioning in 0.01 M $AgNO_3$. The reference electrode was Ag/AgCl/3 M KCl (Metrohm) and the counter electrode was a GC rod. Figure 20 shows the cyclic voltammograms of GC/PEDOT(PSS) electrodes recorded in 0.1 M KNO_3 (Figure 20a) and in 0.1 M KCl solutions (Figure 20b). The red dashed lines represent the cyclic voltammograms of the electrodes before they were conditioned in 0.01 M $AgNO_3$ and the solid blue lines represent the cyclic voltammograms after conditioning in 0.01 M $AgNO_3$.

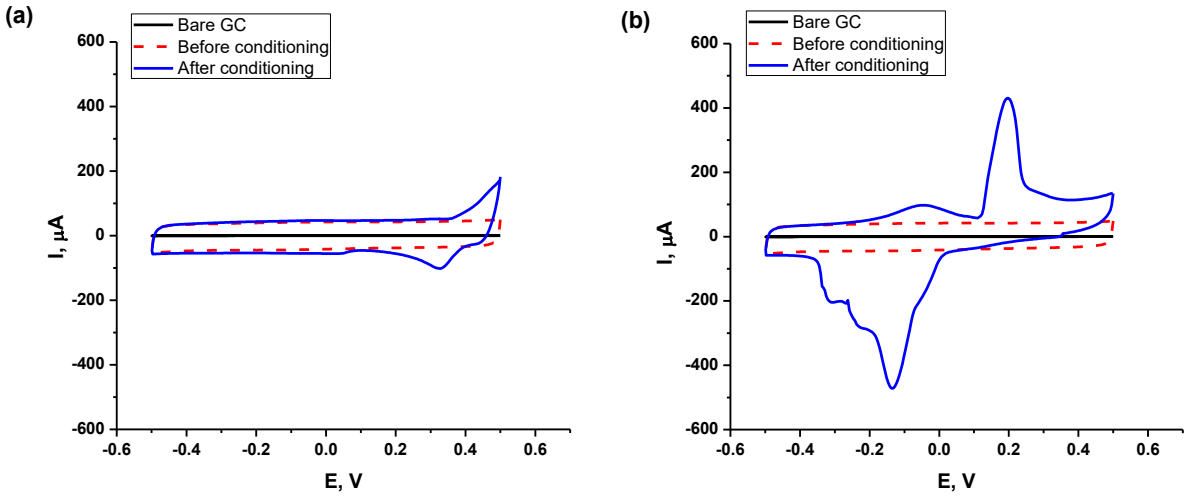

Figure 20. *Cyclic voltammograms (5th cycle) of GC/PEDOT(PSS) electrodes conditioned in 0.01 M $AgNO_3$, recorded in 0.1 M KNO_3 (a) and in 0.1 M KCl solutions (b) at a scan rate of 0.1 V/s.*

The cyclic voltammogram recorded in 0.1 M KNO_3 for the $AgNO_3$-conditioned GC/PEDOT(PSS) electrode (Figure 20a-solid blue line) showed an oxidation peak at ca. 0.45 V which can be assigned to the oxidation of metallic silver inside the polymer film while a corresponding reduction peak occurs at ca. 0.30 V. In an earlier study by Mousavi et al. [43], it was observed

that conditioning the PEDOT film in $AgNO_3$ for a longer period promoted the oxidation of silver during the anodic scan and delayed the reduction of silver in the cathodic scan. This was attributed to the complexation of Ag^+ by the heteroatoms (i.e. oxygen, sulfur) and/or double bonds in the conducting polymer.

On the other hand, Figure 20b (solid blue line) shows the cyclic voltammogram recorded in 0.1 M KCl for the $AgNO_3$-conditioned GC/PEDOT(PSS) electrode. The presence of the main oxidation peak at ca. 0.20 V can be ascribed to the oxidation of silver in the polymer film. The sharp reduction peak at ca. -0.13 V corresponds to the reduction of silver ions. As can be seen in Figure 20b, the oxidation and reduction peaks in the cyclic voltammogram recorded in KCl occurred at lower potentials than those observed in the cyclic voltammogram recorded in KNO_3. This may be explained by considering that the chloride ions can form the sparingly soluble salt with silver (AgCl) in addition to the complexation of Ag^+ by the heteroatoms and double bonds in the film itself. This will therefore promote the oxidation of Ag^0 and delay the reduction of Ag^+.

For the GC/PEDOT(PSS) electrodes conditioned in $AgNO_3$, it can be observed that the magnitude of the currents produced during the anodic and cathodic scans are higher for the cyclic voltammogram recorded in KCl than that recorded in KNO_3. This may be due to the reaction of silver with the chloride ions when KCl was used as supporting electrolyte. The fast consumption of silver ions by the chloride ions resulted in a higher current in the potential scans. These observations show that the supporting electrolyte influences the $Ag^+ + e^- \leftrightharpoons Ag^0$ redox process as well as the shape of the cyclic voltammogram of the $AgNO_3$-conditioned GC/PEDOT(PSS) electrodes. It was shown earlier that the dopant for PEDOT also affects the shape of the cyclic voltammogram [39].

4.2.2. SEM/EDAX measurements

SEM results of the prepared Pt/PEDOT(PSS) electrodes confirm the accumulation of silver in PEDOT(PSS) films after being conditioned in $AgNO_3$. The scanning electron micrograph of PEDOT(PSS) film conditioned in 0.01 M $AgNO_3$ for two days (Figure 21b) show silver particles as bright spots which are absent in the unconditioned PEDOT(PSS) film (Figure 21a) or PEDOT(PSS) film conditioned in KCl (not shown). Silver was not only detected as bright spots but also as scattered grains distributed throughout the entire surface of the film. Elemental

analysis by EDAX also confirms the presence of silver in PEDOT(PSS) films conditioned in 0.01 M $AgNO_3$ (see Table 4). Accumulation of silver was also observed earlier in PEDOT doped with other dopants [39].

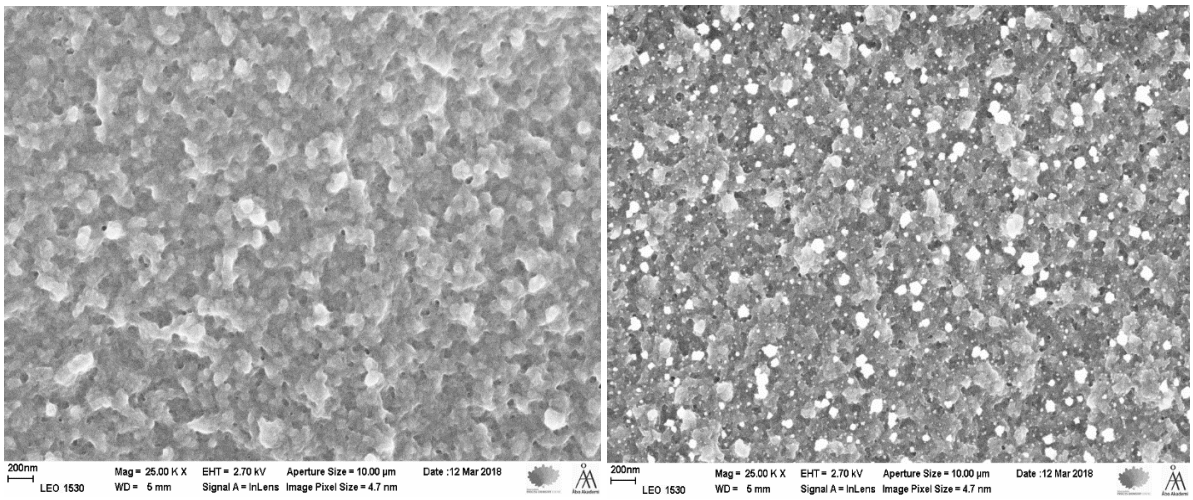

(a) (b)

Figure 21. *Scanning electron micrographs of Pt/PEDOT(PSS) unconditioned (a) and conditioned in 0.01 M $AgNO_3$ for two days (b). The bright spots in (b) are due to the aggregation of silver in the polymer film*.

The elemental composition of the PEDOT(PSS) films obtained from EDAX measurements are summarized in Table 4. Pt/PEDOT(PSS)-1 represents the electrode that was unconditioned and no cyclic voltammogram were recorded for it. The elements present in the PEDOT(PSS) film in this case are oxygen (O), carbon (C), and sulfur (S) which are associated with the PEDOT polymer and polystyrenesulfonate dopant. The Pt/PEDOT(PSS)-2 electrode, which was conditioned in 0.01 M KCl for two days likewise contains O, C, and S in the film but not K. The Pt/PEDOT(PSS)-3 electrode, which was conditioned in 0.01 M $AgNO_3$ for two days and no cyclic voltammograms were recorded for it before EDAX measurement, contained 6.1±0.3% wt silver, which indicates that silver accumulated in the polymer film. In the Pt/PEDOT(PSS)-4 electrode, which was conditioned in 0.01 M $AgNO_3$ for two days and cyclic voltammograms were recorded for it in 0.1 M KCl, the silver content was 2.9±0.4% wt. On the other hand, the Pt/PEDOT(PSS)-5 electrode, which was conditioned in 0.01 M $AgNO_3$ for two days and cyclic voltammograms were recorded for it in 0.1 M KNO_3, contained 8.9±0.5% silver. The standard deviation of the Ag content was obtained from repeated tests on the same sample. The EDAX results show differences in the Ag content of the Pt/PEDOT(PSS) electrodes conditioned in

$AgNO_3$. However ideally, all the Pt/PEDOT(PSS) electrodes conditioned in $AgNO_3$ would have identical amounts of deposited silver as they have the same conditioning period in 0.01 M $AgNO_3$ (2 days). It was earlier observed that for a longer conditioning period in 0.01 M $AgNO_3$, a greater amount of silver was deposited in polypyyrole (PPy) films [39].

Table 4. *EDAX results for the studied Pt/PEDOT(PSS) electrodes. The standard deviation for Ag content was obtained from repeated measurements on the same sample.*

Electrode	Conditioning Solution	Conditioning time	Cyclic voltammogram recorded	Elements detected In the film
Pt/PEDOT(PSS)-1	unconditioned	--	none	O, C, S
Pt/PEDOT(PSS)-2	0.01 M KCl	2 days	none	O, C, S
Pt/PEDOT(PSS)-3	0.01 M $AgNO_3$	2 days	none	O, N, C, S, Ag (6.1±0.3 wt%)
Pt/PEDOT(PSS)-4	0.01 M $AgNO_3$	2 days	in 0.1 M KCl	O, N, C, S, Ag (2.9±0.4 wt%)
Pt/PEDOT(PSS)-5	0.01 M $AgNO_3$	2 days	in 0.1 M KNO_3	O, N, C, S, Ag (8.9±0.5 wt%)

For the EDAX of Pt/PEDOT(PSS) electrodes, two replicates were prepared for each type of Pt/PEDOT(PSS) electrode. The complete elemental composition of all the tested Pt/PEDOT(PSS) electrodes can be found in the appendix of this thesis. Significant differences in the Ag content were observed even in replicate samples. These differences are due to the uneven distribution of silver in the films and the variations in the sample area taken by the instrument for analysis.

4.2.3 Potentiometric measurements

After the characterization by cyclic voltammetry, the GC/PEDOT(PSS) electrodes conditioned in 0.01 M $AgNO_3$ were subjected to potentiometric measurements. Three types of GC/PEDOT(PSS) electrodes were prepared for this experiment: GC/PEDOT(PSS) electrodes with no cyclic voltammogram recorded for them (GC/PEDOT(PSS)-1), GC/PEDOT(PSS) electrodes with cyclic voltammograms recorded in 0.1 M KCl (GC/PEDOT(PSS)-2), and GC/PEDOT(PSS) electrodes with cyclic voltammograms recorded in 0.1 M KNO_3 (GC/PEDOT(PSS)-3). The reference electrode used was a double-junction Ag/AgCl/3M KCl electrode (Metrohm) with a salt bridge containing 1 M LiOAc and calibrations were carried

out using 10^{-1} to 10^{-5} M KCl, $AgNO_3$, KNO_3, Na_2SO_4, NaF, NaBr, NaSCN, $K_2Cr_2O_7$, $NaHCO_3$, and $Na_2C_2O_4$ solutions.

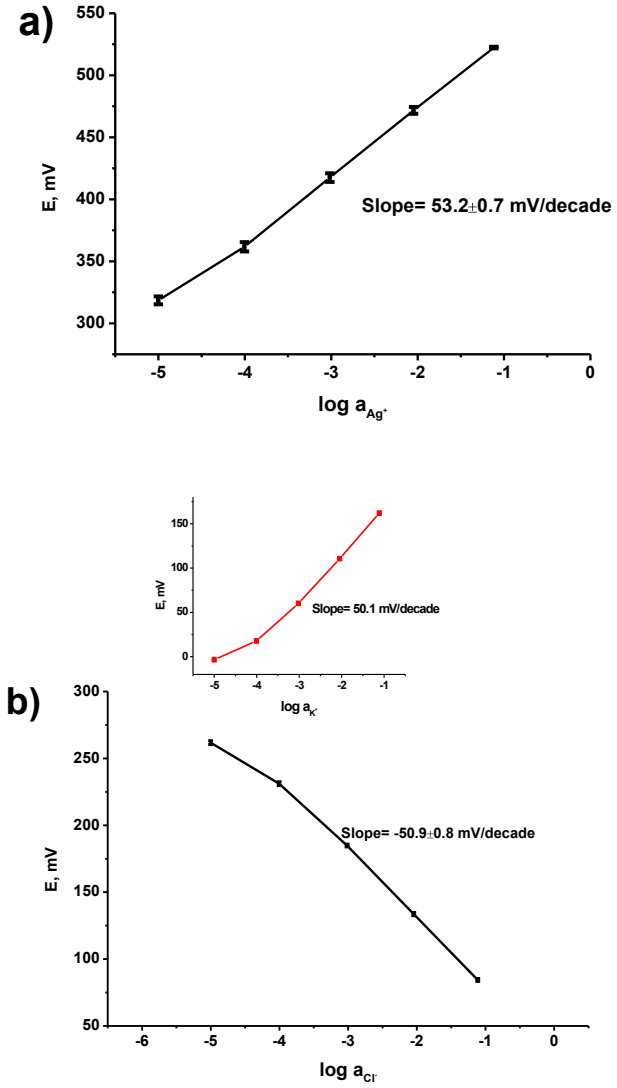

Figure 22. *Calibration of GC/PEDOT(PSS) electrodes (conditioned in 0.01 M $AgNO_3$) carried out in 10^{-1} to 10^{-5} M $AgNO_3$ solutions (a) and in 10^{-1} to 10^{-5} M KCl solutions (b). In (b), the inserted figure corresponds to the calibration curve for the GC/PEDOT(PSS) electrode in KCl solutions prior to conditioning in $AgNO_3$. The error bars correspond to the standard deviation of the measured potentials for the same electrode on different days of calibration. The total conditioning time was 7-11 days (see Table 5)*

Figure 22 shows typical calibration curves of the $AgNO_3$-conditioned GC/PEDOT(PSS) electrodes in $AgNO_3$ and KCl solutions. The GC/PEDOT(PSS) electrodes showed a cationic response when calibrated in $AgNO_3$ solutions (Figure 22a) which means that the electrodes were sensitive towards the silver ion. On the other hand, when the $AgNO_3$-conditioned GC/PEDOT(PSS) electrodes were calibrated in KCl solutions, an anionic response was observed

(Figure 22b), which indicates sensitivity toward chloride ion. Prior to conditioning in 0.01 M $AgNO_3$ solution, the GC/PEDOT(PSS) electrodes have cationic response in KCl solutions (Figure 22b - inset) which indicates sensitivity towards K^+ ion. The reversal of potentiometric response is evidently influenced by the deposition of silver in the PEDOT(PSS) film which occurs spontaneously upon conditioning in $AgNO_3$ solution, as shown by EDAX and cyclic voltammetry measurements. Table 5 summarizes the slope values and the linear ranges obtained from calibrations carried out in $AgNO_3$ and KCl solutions for the three types of GC/PEDOT(PSS) electrodes prepared:

Table 5. *Calibration data for the three types of GC/PEDOT(PSS) conditioned in 0.01 M $AgNO_3$. The standard deviation indicates the variations in the calibration parameters obtained for the same electrode during different days of calibration.*

Electrode	CV after conditioning in $AgNO_3$	Standard potential (E^o) ± *SD* (mV)	Slope ± SD (mV/decade)	Linear Range (M)
Calibration in $AgNO_3$ solutions				
GC/PEDOT(PSS)-1*	none	573.1 ± 3.4	51.3 ± 1.8	10^{-1}-10^{-5}
GC/PEDOT(PSS)-2**	in 0.1 M KCl	580.0 ± 0.8	53.2 ± 0.7	10^{-1}-10^{-5}
GC/PEDOT(PSS)-3**	in 0.1 M KNO_3	576.4 ± 4.4	49.7 ± 1.0	10^{-1}-10^{-5}
Calibration in KCl solutions				
GC/PEDOT(PSS)-1*	none	41 ± 12	-46.9 ± 3.1	10^{-1}-10^{-4}
GC/PEDOT(PSS)-2**	in 0.1 M KCl	28.9 ± 2.3	-50.9 ± 0.8	10^{-1}-10^{-4}
GC/PEDOT(PSS)-3**	in 0.1 M KNO_3	30.4 ± 2.6	-49.8 ± 0.8	10^{-1}-10^{-4}

* calibrations done on the 3rd, 5th and 11th days of conditioning in 0.01 M $AgNO_3$
** calibrations done on the 5th, 6th and 7th days of conditioning in 0.01 M $AgNO_3$

It can be seen from Table 5 that the slopes of the GC/PEDOT(PSS) electrodes conditioned in $AgNO_3$ were close to Nernstian in the activity range of 10^{-1}-10^{-5} M of Ag^+ in the case of calibrations carried out in $AgNO_3$ solutions. The standard deviation of E^o was lowest for GC/PEDOT(PSS)-2 for which cyclic voltammograms were recorded in 0.1 M KCl solution.

For calibrations carried out in KCl solutions, the slope values range from -47 to -51 mV/decade within a linear range of 10^{-1} to 10^{-4} M KCl for all the prepared GC/PEDOT(PSS) electrodes (Table 5). Deviations in E^o values were smaller for GC/PEDOT(PSS)-2 and GC/PEDOT(PSS)-3 electrodes compared to the GC/PEDOT(PSS)-1 electrode for which no cyclic voltammogram was

recorded. The observed sensitivity towards Cl^- may be due to the tendency of chloride ions to form a salt with Ag^+.

The potentiometric response of the GC/PEDOT(PSS) electrodes conditioned in $AgNO_3$ was also tested in various solutions and are illustrated in Figure 23. For each type of GC/PEDOT(PSS) electrode, two replicates were prepared. The complete potentiometric data obtained for all the prepared electrodes in the studied solutions can be found in the appendix of this thesis. As can be seen in Figure 23, the potentiometric response of the electrodes in Na_2SO_4, NaF, $NaHCO_3$, $Na_2C_2O_4$, KNO_3, and $K_2Cr_2O_7$ solutions was cationic (Figure 23a) indicating that the electrodes were sensitive towards Na^+ or K^+. On the other hand, the electrode response in KCl, KI, NaBr, and NaSCN solutions was anionic (Figure 23b) which means that the electrodes were sensitive to the anions present in the solutions. As with chloride ions, the anionic response of the GC/PEDOT(PSS) electrodes conditioned in $AgNO_3$ can be associated with the silver present in the film that can form a salt with the anions (Br^-, I^-, and SCN^-).

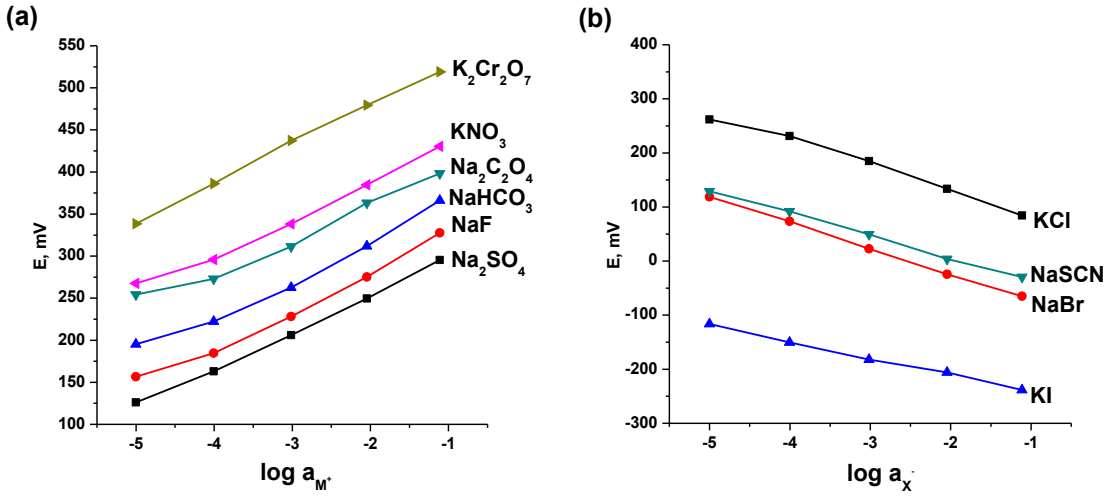

Figure 23. *Cationic (a) and anionic (b) response of the $AgNO_3$-conditioned GC/PEDOT(PSS) electrodes measured in various solutions. In (a), the potential values of the calibration curves for NaF, $NaHCO_3$, $Na_2C_2O_4$ and KNO_3 were shifted by +30, +60, +90 and +120 mV respectively to avoid the overlap of the calibration curves.*

Table 6 shows the list of calibrations solutions wherein anionic response was observed for the GC/PEDOT(PSS) electrodes conditioned in $AgNO_3$. It can be observed that the typical slopes obtained for the calibration solutions vary from one solution to another. All the anions in the studied salt solutions (Cl^-, Br^-, I^- and SCN^-) have the ability to form insoluble salts with Ag^+. Interestingly, for the halide anions (Cl^-, Br^-, and I^-), the slope values appear to correlate with

the K_{sp} values of their silver salts (AgCl, AgBr and AgI). The slope of the calibration curve for KCl (-50.9 mV/decade) was closest to Nernstian followed by NaBr (-47.8 mV/decade), then KI (-30.7 mV/decade). The magnitude of the K_{sp} of the silver salts follow the same order with AgCl having the highest K_{sp} (i.e. most soluble) (1.8×10^{-10}), followed by AgBr (5.0×10^{-13}) then AgI (8.3×10^{-17}). This observed behavior is worthy of further study.

Table 6. *Calibration data of $AgNO_3$-conditioned GC/PEDOT(PSS) electrodes in solutions where anionic response was observed. K_{sp} (AgX) refers to the solubility product constant of the silver salt with the different anions in the calibration solutions.*

Calibration Solution	Linear range	Slope, mV/decade	K_{sp} (AgX)	pK_{sp} (AgX)
KCl	10^{-1}-10^{-4}	-50.9	1.8×10^{-10}	9.74
NaBr	10^{-1}-10^{-5}	-47.8	5.0×10^{-13}	12.30
KI	10^{-1}-10^{-5}	-30.7	8.3×10^{-17}	16.08
NaSCN	10^{-1}-10^{-5}	-41.5	1.1×10^{-12}	11.97

4.3. Assessment of E^o stability of K^+-ISEs with Ag-deposited PEDOT(PSS) films as solid-contact

The effect of silver deposition in the PEDOT(PSS) film on the standard potential stability of GC/PEDOT(PSS)/K^+-ISM was evaluated using conventional calibrations in KCl solutions. The reference electrode used was a double-junction Ag/AgCl/3M KCl electrode (Metrohm) with a salt bridge containing 1M LiOAc and calibrations were carried out in 10^{-1}-10^{-7} M KCl solutions. As a convention, GC/PEDOT(PSS)/K^+-ISM-1 refers to GC/PEDOT(PSS)/K^+-ISM electrode in which no cyclic voltammogram was recorded for GC/PEDOT(PSS), GC/PEDOT(PSS)/K^+-ISM-2 and GC/PEDOT(PSS)/K^+-ISM-3 indicate electrodes in which cyclic voltammograms were recorded for GC/PEDOT(PSS) in 0.1 M KCl and 0.1 M KNO_3, respectively. For all the studied GC/PEDOT(PSS)/K^+-ISM electrodes, 3 replicates were prepared. Figure 24 shows the cumulative calibration curves of the GC/PEDOT(PSS)/K^+-ISM electrodes with the lowest E^o standard deviation for each type in 10^{-1}-10^{-7} M KCl solutions for the entire conditioning periods in 0.01 M KCl.

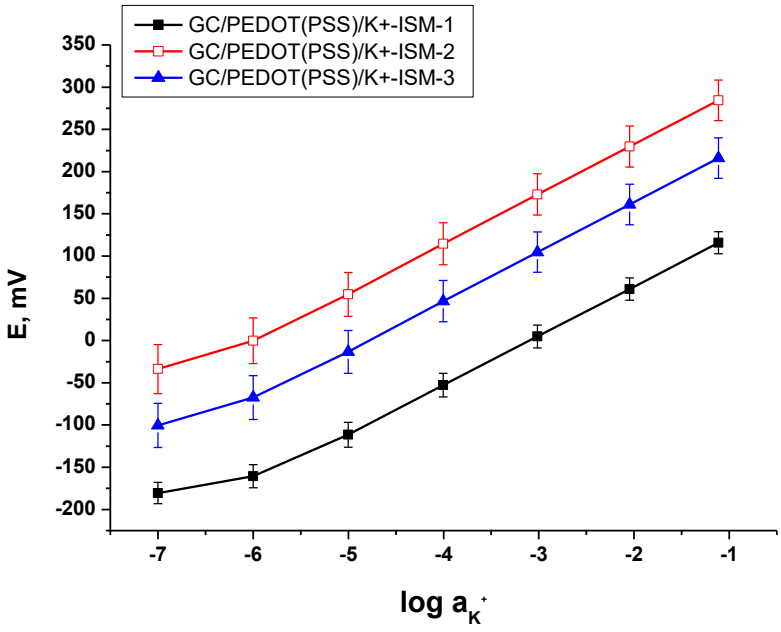

Figure 24. *Calibration curves for GC/PEDOT(PSS)/K^+-ISM-1, GC/PEDOT(PSS)/K^+-ISM-2, and GC/PEDOT(PSS)/K^+-ISM-3 electrodes in 10^{-1} to 10^{-7} M KCl solutions. The error bars on the calibration curves correspond to the standard deviations of the measured potentials for the same electrodes during several weeks of repeated calibrations. The potentials for GC/PEDOT(PSS)/K^+-ISM-3 were shifted by -50 mV for better visualization. All the GC/PEDOT(PSS) electrodes were conditioned in 0.01 M $AgNO_3$ before applying the K^+-ISM.*

As can be observed in Figure 24, all the studied GC/PEDOT(PSS)/K^+-ISM electrodes have a linear response in the activity range 10^{-1}-10^{-6} M KCl. The error bars on each calibration curve indicate the standard deviations of the measured electrode potentials for the same electrode during several weeks of repeated calibrations. The smallest deviations in electrode potentials were observed for the GC/PEDOT(PSS)/K^+-ISM-1 electrode in which no cyclic voltammogram was recorded for GC/PEDOT(PSS).

The inter-day changes in E^o for the same electrodes studied in Figure 24 are illustrated in Figure 25. It can be observed that for all the analyzed GC/PEDOT(PSS)/K^+-ISM electrodes, there was a shift towards lower E^o values upon prolonged conditioning. This behavior is different to that observed for the GC/PEDOT(PSS)/K^+-ISM electrode in which the GC/PEDOT(PSS) was not conditioned in $AgNO_3$ (Figure 18a), where the shift was towards higher E^o values. Therefore conditioning of the GC/PEDOT(PSS) electrodes in $AgNO_3$ had an effect on the potentials of the GC/PEDOT(PSS)/K^+-ISM electrodes studied in this experiment. Furthermore, the E^o values of

the GC/PEDOT(PSS)/K^+-ISM electrodes shown in Figure 25 did not stabilize throughout the entire conditioning period. This may also be brought about by the deposition of silver on the PEDOT(PSS) films.

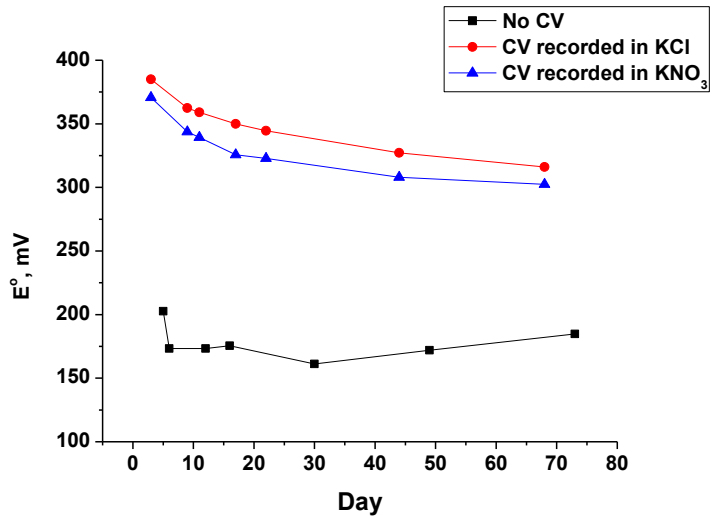

Figure 25. *Plots of the standard potentials (E^o) for the GC/PEDOT(PSS)/K^+-ISM electrodes with Ag-deposited PEDOT(PSS) films on different days of calibration in KCl solutions.*

Table 7 summarizes the calibration data obtained for GC/PEDOT(PSS)/K^+-ISM-1, GC/PEDOT(PSS)/K^+-ISM-2, and GC/PEDOT(PSS)/K^+-ISM-3 electrodes in their respective periods of conditioning in 0.01 M KCl. The values reflected for each electrode type corresponds to the electrode with the lowest E^o standard deviation among three identically prepared electrodes. The calibration data for all the prepared electrodes can be found in the appendix. The performance of a commercial K^+-ISE (Thermo Scientific Orion) was tested alongside the fabricated K^+-ISEs for comparison.

Table 7. *Calibration data for the three types of GC/PEDOT(PSS)/K^+-ISM prepared. The standard deviation indicates the variations in the calibration parameters obtained for the same electrode during different days of calibration.*

Electrode	Conditioning time	CV after conditioning in $AgNO_3$	Standard potential (E^o) ± SD (mV)	Slope ± SD (mV/decade)	Linear Range (M)
GC/PEDOT(PSS)/K^+-ISM-1	73	none	178 ± 13	57.1 ± 0.7	10^{-1}-10^{-6}
GC/PEDOT(PSS)/K^+-ISM -2	68	in 0.1 M KCl	349 ± 23	58.5 ± 0.7	10^{-1}-10^{-6}
GC/PEDOT(PSS)/K^+-ISM -3	68	in 0.1 M KNO_3	330 ± 23	58.3 ± 0.6	10^{-1}-10^{-6}
Commercial K^+-ISE*	--	--	90.1 ± 2.4	57.6 ± 0.4	10^{-1}-10^{-5}

* no conditioning required in-between calibrations

As can be seen from Table 7, GC/PEDOT(PSS)/K^+-ISM-1 has the lowest standard deviation of E^o (± 13mV) and therefore the highest E^o stability. The GC/PEDOT(PSS)/K^+-ISM-2 and GC/PEDOT(PSS)/K^+-ISM-3 both have an E^o standard deviation of ± 23 mV. These results show that performing cyclic voltammetry for $AgNO_3$-conditioned GC/PEDOT(PSS) electrodes prior to applying K^+-ISM did not improve the stability of the standard potential. Furthermore, comparing the GC/PEDOT(PSS)/K^+-ISM electrodes in which the GC/PEDOT(PSS) was conditioned in $AgNO_3$ before applying K^+-ISM (Table 7) to that in which the GC/PEDOT(PSS) was conditioned in KCl before applying K^+-ISM (see Table 3), there is no improvement in E^o stability in the GC/PEDOT(PSS)/K^+-ISM with Ag-deposited GC/PEDOT(PSS). This behavior may be due to the effect of silver on the interfacial potential between the ion-selective membrane and the conducting polymer. For the GC/PEDOT(PSS)/K^+-ISM electrodes studied in this experiment, a shift to more negative E^o values (see Figure 25) at longer periods of conditioning was also observed. This may be due to the affinity of the Ag-deposited PEDOT(PSS) film to the chloride ions in the calibration solution.

4.4. Characterization of solid-contact Cl^--ISEs and assessment of E^o stability

4.4.1. CV and EIS measurements

Cyclic voltammograms of GC/PEDOT(Cl) were recorded in 0.1 M KCl in the potential range of -0.5 to 0.5 V at a scan rate of 0.1 V/s. The resulting cyclic voltammogram is similar to that shown in Figure 12 for GC/PEDOT(Cl). EIS measurements were also carried out for GC/PEDOT(Cl) and GC-AuNPs/PEDOT(Cl) electrodes using the procedure described in section 3.6. The impedance spectra obtained for GC/PEDOT(Cl) and GC-AuNPs/PEDOT(Cl) electrodes were identical to those illustrated in Figure14a for GC/PEDOT(Cl) and Figure 14b for GC-AuNPs/PEDOT(Cl). The C_{LF} values were determined at the lowest frequency used to record the spectra (0.01 Hz) using Equation 14. The obtained C_{LF} values were 307 µF for GC/PEDOT(Cl) and 363 µF for GC-AuNPs/PEDOT(Cl).

After applying Cl^--ISM on the GC/PEDOT(Cl) and GC-AuNPs/PEDOT(Cl) electrodes, the impedance spectra of GC/PEDOT(Cl)/Cl^--ISM and GC-AuNPs/PEDOT(Cl)/Cl^--ISM electrodes were recorded in 0.1 M KCl at 100 KHz-10 mHz. The resulting impedance spectra for GC/PEDOT(Cl) and GC-AuNPs/PEDOT(Cl) are shown in Figure 26.

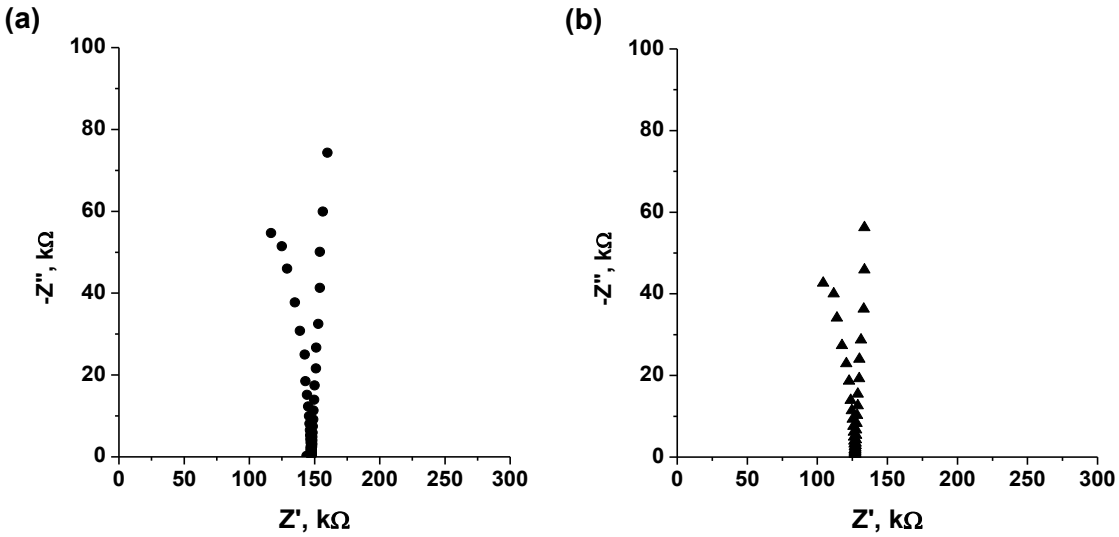

Figure 26. *Impedance spectra of GC/PEDOT(Cl)/ Cl^--ISM (a) and GC-AuNPs/PEDOT(Cl)/Cl^--ISM (b) recorded in 0.1 M KCl at ΔE_{ac} = 10 mV. The frequency range was 100 KHz-10 mHz.*

The impedance spectra of both GC/PEDOT(Cl)/Cl^--ISM (Figure 26a) and GC-AuNPs/PEDOT(Cl)/Cl^--ISM (Figure 26b) electrodes show a low-frequency capacitive line and a high-frequency charge-transfer semicircle [44]. Compared to the GC/PEDOT(Cl)/K^+-ISM and GC-AuNPs/PEDOT(Cl)/K^+-ISM electrodes, the bulk resistance for GC/PEDOT(Cl)/Cl^--ISM (~ 150 kΩ) and GC-AuNPs/PEDOT(Cl)/Cl^--ISM (~ 125 kΩ) are much lower. This is due to the lower bulk resistance of the Cl^--ISM than the K^+-ISM.

4.4.2. Potentiometric measurements

Prior to applying the Cl^--ISM, the prepared GC/PEDOT(Cl), GC-AuNPs/PEDOT(Cl), and Ag/AgCl electrodes were subjected to potentiometric measurements using 10^{-1}-10^{-6} M KCl solutions. The reference electrode used was Ag/AgCl/3M KCl (Metrohm) with a salt bridge containing 1M LiOAc. Calibration plots for the GC/PEDOT(Cl), GC-AuNPs/PEDOT(Cl), and Ag/AgCl electrodes are shown in Figure 27 and the obtained calibration data are summarized in Table 8.

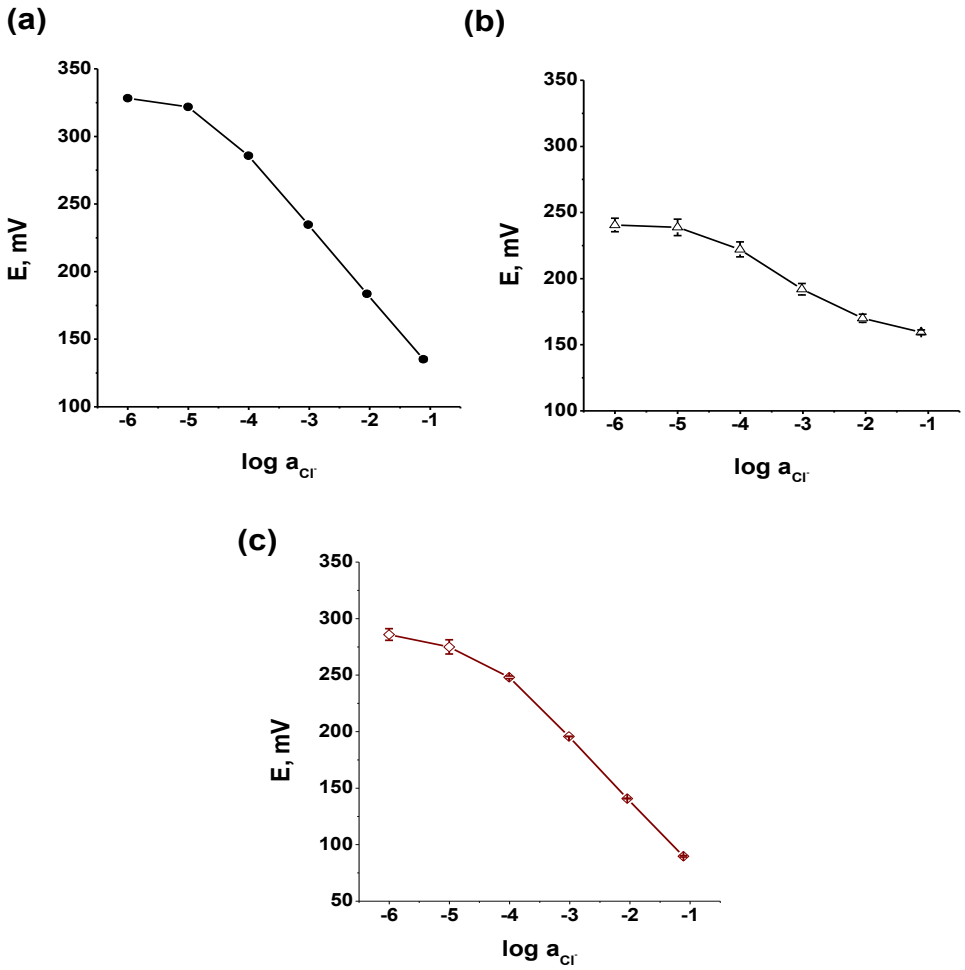

Figure 27. *Calibration plots for GC/PEDOT(Cl) (a), GC-AuNPs/PEDOT(Cl) (b), and Ag/AgCl (c) electrodes in 10^{-1}-10^{-6} M KCl solutions. The error bars on the calibration curves correspond to the standard deviations of the measured potentials for the same electrodes during different days of repeated calibrations (see Table 8).*

As shown in Figure 27, the potentiometric responses of GC/PEDOT(Cl), GC-AuNPs/PEDOT(Cl), and Ag/AgCl electrodes were anionic. The error bars in the calibration curves indicate the standard deviation of the measured potentials for the same electrodes during certain days of measurement (see Table 8). The calibration curve for the GC-AuNPs/PEDOT(Cl) electrode was less linear than that for the GC/PEDOT(Cl) electrode as was explained in section 4.1.2.

Table 8. *Calibration data of GC/PEDOT(Cl), GC-AuNPs/PEDOT(Cl) and Ag/AgCl electrodes in 10^{-1}-10^{-6} M KCl solutions. The standard deviation indicates the variations in the calibration parameters obtained for the same electrode during different days of calibration*.

Electrode	Standard potential (E^o) ± SD (mV)	Slope ± SD (mV/decade)	Linear Range (M)
GC/PEDOT(Cl)*	77.2 ± 1.7	-52.1 ± 0.2	10^{-1}-10^{-4}
Ag/AgCl**	28.8 ± 1.4	-54.9 ± 0.6	10^{-1}-10^{-4}
GC-AuNPs/PEDOT(Cl)***	--	--	--

* calibrations done on the 2nd and 4th days of conditioning in 0.01 M KCl
** calibrations done on the 5th, 6th and 7th days of conditioning in 0.01 M KCl
*** non-linear potentiometric response

As listed in Table 8, the linear responses of both GC/PEDOT(Cl) and Ag/AgCl electrodes were in the activity range of 10^{-1}-10^{-4} M of Cl^-. The slope of the calibration curve for GC/PEDOT(Cl) was -52.1 ± 0.2 mV/decade while that of Ag/AgCl was -54.9 ± 0.6 mV/decade. The standard deviation of E^o was comparable for the two electrodes, with ± 1.7 mV for GC/PEDOT(Cl) and ± 1.4 mV for Ag/AgCl.

4.4.3. Chronopotentiometry

After applying the Cl^--ISM on the GC/PEDOT(Cl) and GC-AuNPs/PEDOT(Cl) electrodes and subsequent conditioning, the potential stability of the GC/PEDOT(Cl)/Cl^--ISM and GC-AuNPs/PEDOT(Cl)/Cl^--ISM electrodes was studied using chronopotentiometry. The chronopotentiometric method used for the solid-contact Cl^--ISEs was the same as for the solid-contact K^+-ISEs (see section 3.7). The obtained chronopotentiograms for GC/PEDOT(Cl)/Cl^--ISM and GC-AuNPs/PEDOT(Cl)/Cl^--ISM are shown in Figure 28.

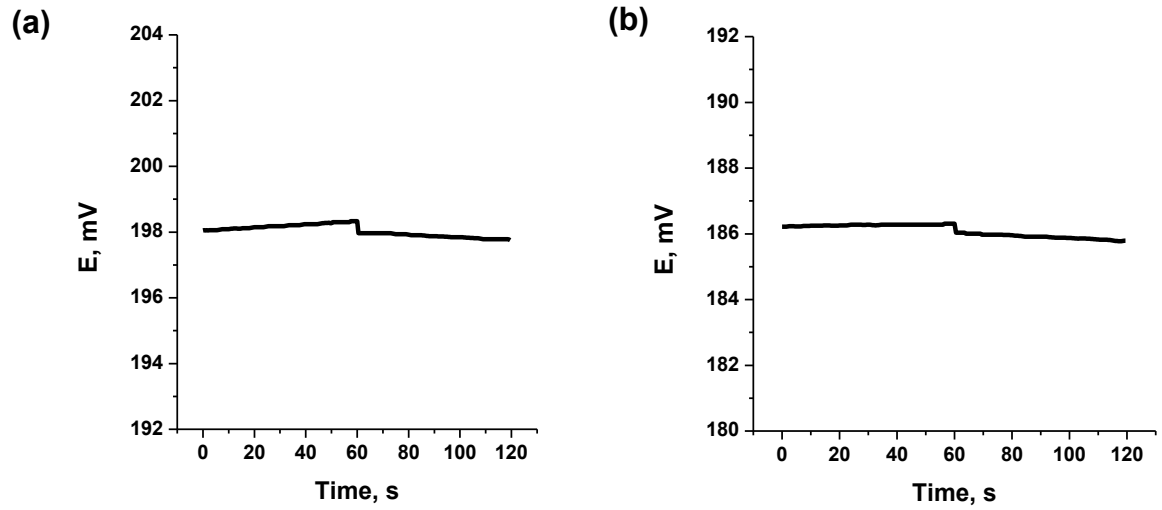

Figure 28. *Chronopotentiograms of GC/PEDOT(Cl)/Cl^--ISM (a) and GC-AuNPs/PEDOT(Cl)/Cl^--ISM (b) recorded in 0.1 M KCl solution. Applied current is +1 nA for 60 s and -1 nA for 60s.*

The chronopotentiograms of the GC/PEDOT(Cl)/Cl^--ISM and GC-AuNPs/PEDOT(Cl)/Cl^--ISM electrodes showed a potential jump when the applied current changed from +1 nA to -1 nA. However, potential jumps were significantly smaller compared to the case of solid-contact K^+-ISEs (section 4.1.4). The R_T estimated from the potential jump using Equation 15 was 155 kΩ for GC/PEDOT(Cl)/Cl^--ISM and 120 kΩ for GC-AuNPs/PEDOT(Cl)/Cl^--ISM. These values are in good agreement with the bulk resistance estimated from EIS measurements (see Figure 26).

The potential drift of the GC/PEDOT(Cl)/Cl^--ISM and GC-AuNPs/PEDOT(Cl)/Cl^--ISM electrodes were evaluated from the slopes ($\Delta E/\Delta t$) of the E-t curves at longer times. The low-frequency capacitance (C_{LF}) for both electrodes were then calculated from the potential drift using Equation 16. The obtained results are summarized in Table 9.

Table 9. *Results from chronopotentiometric measurements carried out for GC/PEDOT(Cl)/Cl^--ISM and GC-AuNPs/PEDOT(Cl)/Cl^--ISM electrodes.*

Electrode	$\Delta E/\Delta t$ (μV/s)	C_{LF} (μF)
GC/PEDOT(Cl)/Cl^--ISM	4.6	217
GC-AuNPs/PEDOT(Cl)/Cl^--ISM	3.7	270

The C_{LF} values obtained from chronopotentiometry are lower than those calculated for the GC/PEDOT(Cl) and GC-AuNPs/PEDOT(Cl) electrodes from EIS experiments due to the coverage Cl^- selective membrane. This behavior is similar to those observed in solid-contact K^+-ISEs (see Table 2) which proves that the ion-transport to/from the polymer film is more efficient in an electrolyte medium than in a PVC membrane.

4.4.4. Evaluation of E^o stability

The stability of the standard potential (E^o) of the GC/PEDOT(Cl)/Cl^--ISM, GC-AuNPs/PEDOT(Cl)/Cl^--ISM, and Ag/AgCl/Cl^--ISM electrodes was studied using conventional calibrations in 10^{-1}-10^{-7} M KCl solutions. The reference electrode was Ag/AgCl/3M KCl (Metrohm) with a salt bridge containing 1 M LiOAc. The standard potential (E^o) was determined as the y-intercept of the linear part of the calibration curve. The calibrations were repeated for several weeks and the electrodes were kept conditioned in 0.01 M KCl in between calibrations. The stability of E^o was evaluated as the standard deviation of the experimental E^o values obtained from all the calibrations carried out for each electrode.

Figure 29 shows the changes in E^o values for the GC/PEDOT(Cl)/Cl^--ISM, GC-AuNPs/PEDOT(Cl)/Cl^--ISM, and Ag/AgCl/Cl^--ISM electrodes during their respective conditioning periods. For all the studied solid-contact Cl^--ISEs, there was a shift towards more negative standard potentials (E^o) which tended to stabilize at later periods of conditioning. The drop in the E^o values was more significant for the GC/PEDOT(Cl)/Cl^--ISM and GC-AuNPs/PEDOT(Cl)/Cl^--ISM electrodes than for the Ag/AgCl/Cl^--ISM electrode. In an earlier study by Maj-Żurawska et al. [45], solid-state planar miniature Cl^--ISEs with polypyrrole doped with hexacyanoferrate (II) ions (PPyFeCN) as solid-contact, also showed potential drifts during the first 3 days of immersion in 10^{-1} and 10^{-3} M KCl solutions. After this period, the electrode potentials became more stable (± 20 mV) in 10^{-1} and 10^{-3} M KCl solutions for 80 days. In another study, solid-state Cl^--ISEs with a membrane constructed by incorporating trihexadecyl-methylammonium chloride (anion-exchanger salt) into a poly(3-octylthiophene) matrix, gave an average potential of 425 mV in 10^{-1} M KCl which shifted to an average potential of 453 mV after 5 days of conditioning in the same solution [46]. PEDOT was previously used as solid contact in a Cl^--ISE with a PVC-based ISM containing tridodecylmethylammonium chloride (TDMACl) as anion-exchanger [44]. The resulting Cl-ISEs were observed to have highly

reversible ion-to-electron transduction and low hysteresis during calibration in KCl solutions, however, the stability of the electrode potentials were not studied.

The E^o values for GC/PEDOT(Cl)/Cl^--ISM and GC-AuNPs/PEDOT(Cl)/Cl^--ISM started to stabilize after 6 days of conditioning while the E^o values for Ag/AgCl/Cl^--ISM stabilized after 18 days of conditioning. To compare the E^o stability for all the solid-contact Cl^--ISEs studied, the calibration data after 6 days of conditioning were used. All the other calibration parameters measured after 6 days of conditioning were compared.

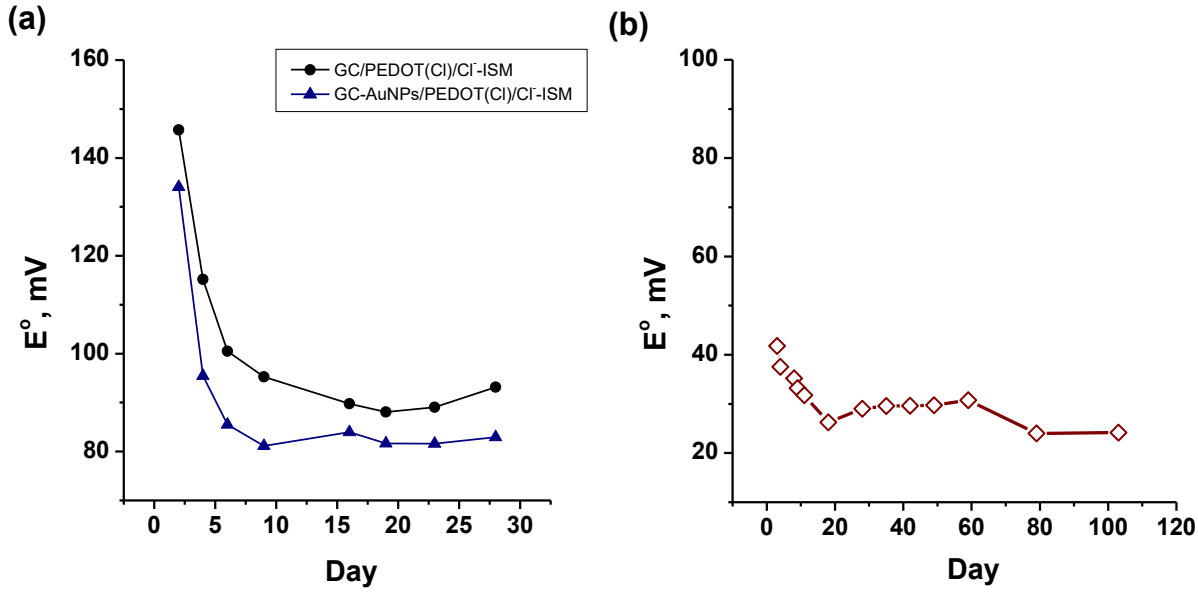

Figure 29. *Plots of standard potentials (E^o) for the GC/PEDOT(Cl)/Cl^--ISM, GC-AuNPs/PEDOT(Cl)/Cl^--ISM (a), and Ag/AgCl/Cl^--ISM electrodes (b) at different days of calibration in KCl solutions. For the E^o stability evaluation, the E^o values after 6 days of conditioning were used.*

The cumulative calibration curves obtained for the the GC/PEDOT(Cl)/Cl^--ISM, GC-AuNPs/PEDOT(Cl)/Cl^--ISM, and Ag/AgCl/Cl^--ISM electrodes after 6 days of conditioning are shown in Figure 30. As can be seen from Figure 30a, the linear part of the calibration curves of the GC/PEDOT(Cl)/Cl^--ISM and GC-AuNPs/PEDOT(Cl)/Cl^--ISM electrodes were in the activity range 10^{-1}-10^{-4} M of Cl^-. Similarly, the linear activity range for the Ag/AgCl/Cl^--ISM electrode (Figure 30b) was 10^{-1} to 10^{-4} M of the Cl^- ion. The error bars in the calibration curves indicate the standard deviations of the potentials from the mean value for the same electrode during different days of calibration. The standard deviations of the measured potentials are

comparable for the GC/PEDOT(Cl)/Cl^--ISM, GC-AuNPs/PEDOT(Cl)/Cl^--ISM, and Ag/AgCl/Cl^--ISM electrodes within their linear activity ranges.

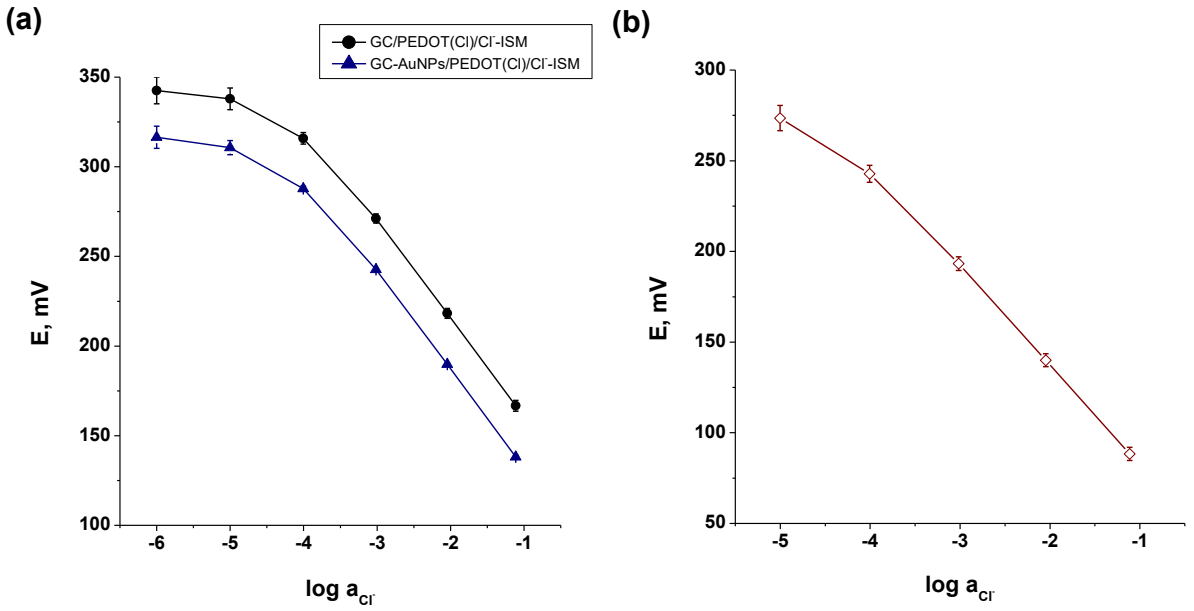

Figure 30. *Calibration curves for the GC/PEDOT(Cl)/Cl^--ISM, GC-AuNPs/PEDOT(Cl)/Cl^--ISM (a), and Ag/AgCl/Cl^--ISM (b) electrodes obtained from calibration data after 10 days of conditioning. The error bars on the calibration curves correspond to the standard deviations of the measured potentials for the same electrodes during the several weeks of repeated calibration.*

Table 10 summarizes the calibration data for the GC/PEDOT(Cl)/Cl^--ISM, GC-AuNPs/PEDOT(Cl)/Cl^--ISM, and Ag/AgCl/Cl^--ISM electrodes after 6 days of conditioning. The parameter values reflected in Table 10 correspond to the electrodes with the lowest E^o standard deviations among three identical electrodes prepared for each electrode type. The calibration data for all the solid-contact Cl^--ISEs prepared for this experiment can be found in the appendix of this thesis. The performance of a commercial chloride ISE (Thermo Scientific Orion 9417BN) is included in Table 10 for comparison. As shown in Table 10, the standard deviation of E^o for GC/PEDOT(Cl)/Cl^--ISM (± 3.0 mV) was higher than that for GC-AuNPs/PEDOT(Cl)/Cl^--ISM (± 1.2 mV) under a conditioning period of 28 days. Both GC/PEDOT(Cl)/Cl^--ISM and GC-AuNPs/PEDOT(Cl)/Cl^--ISM electrodes have a linear activity range of 10^{-1}-10^{-4} M of Cl^-. The slope of the linear part of the calibration curve for GC/PEDOT(Cl)/Cl^--ISM was -51.8 ± 0.5 mV/decade while that for GC-AuNPs/PEDOT(Cl)/Cl^--ISM was -52.0 ± 0.5 mV/decade. On the other hand, the standard deviation of E^o for the Ag/AgCl/Cl^-

-ISM electrode was ± 3.7 mV for the conditioning period of 103 days. The linear activity range for Ag/AgCl/Cl^--ISM was 10^{-1}-10^{-4} M of Cl^- with a slope of -53.5 ± 0.9 mV/decade.

Table 10. *Calibration data for the fabricated solid-contact Cl^--ISEs and a commercial Cl^--ISE obtained after 6 days of conditioning in 0.01 M KCl. The standard deviation indicates the variations in the calibration parameters obtained for the same electrode during different days of calibration.*

Electrode	Conditioning time (day)	Standard potential (E^o) ± SD (mV)	Slope ± SD (mV/decade)	Linear Range (M)
GC/PEDOT(Cl)/Cl^--ISM	28	91.1 ± 3.0	-51.8 ± 0.5	10^{-1}-10^{-4}
GC-AuNPs/PEDOT(Cl)/Cl^--ISM	28	82.3 ± 1.2	-52.0 ± 0.5	10^{-1}-10^{-4}
Ag/AgCl/Cl-ISM	103	29.9 ± 3.7	-53.5 ± 0.9	10^{-1}-10^{-4}
Commercial Cl^--ISE*	--	22.9 ± 3.6	-54.9 ± 0.5	10^{-1}-10^{-4}

* no conditioning required in-between calibrations

Results from this experiment show that the E^o stability was higher when gold nanoparticles-modified glassy carbon (GC-AuNPs) was used as conducting substrate than glassy carbon (GC) for solid-contact Cl^--ISEs based on PEDOT. The potential drift of the GC-AuNPs/PEDOT(Cl)/Cl^--ISM electrode was also lower than GC/PEDOT(Cl)/Cl^--ISM as shown in the chronopotentiometric measurements. This behavior was also observed in the case of GC/PEDOT(Cl)/K^+-ISM and GC-AuNPs/PEDOT(Cl)/K^+-ISM (see Table 3). Therefore the presence of gold nanoparticles in the glassy carbon improved the stability of the ion-to-electron transduction in the solid-contact ISEs studied in this thesis. However, the Ag/AgCl/Cl^--ISM electrode showed good E^o stability for a longer period of conditioning than the GC/PEDOT(Cl)/Cl^--ISM or GC-AuNPs/PEDOT(Cl)/Cl^--ISM electrodes.

5. Conclusions

Poly(3,4-ethylenedioxythiophene) (PEDOT) was electrochemically synthesized using poly(styrene sulfonate) (PSS^-) or chloride (Cl^-) as doping ions. The resulting PEDOT(PSS) and PEDOT(Cl) composites were used as solid-contacts in solid-state K^+-selective electrodes with PVC-based K^+-selective membrane. Cyclic voltammetry measurements of GC/PEDOT(PSS) and GC/PEDOT(Cl) electrodes showed comparable redox capacitance between the PEDOT(PSS) and PEDOT(Cl) films. EIS measurements of GC/PEDOT(PSS) and GC/PEDOT(Cl) electrodes also yielded comparable low-frequency capacitance (C_{LF}) for the two polymer films. From chronopotentiometric measurements, good potential stability was observed for both GC/PEDOT(PSS)/K^+-ISM and GC/PEDOT(Cl)/K^+-ISM electrodes. The stability of the standard potential (E^o) was evaluated from repeated calibrations during extended periods of conditioning. From calibrations carried out after 10 days of conditioning, GC/PEDOT(Cl)/K^+-ISM showed better E^o stability than GC/PEDOT(PSS)/K^+-ISM under a conditioning period of 103 days. The results suggest that E^o stability is better for the K^+-ISE with PEDOT(Cl) as solid-contact than that with PEDOT(PSS) as solid-contact.

The effect of using gold nanoparticles-modified glassy carbon (GC-AuNPs) as conducting substrate was also studied. From calibrations carried out after 10 days of conditioning, the GC-AuNPs/PEDOT(PSS)/K^+-ISM and GC-AuNPs/PEDOT(Cl)/K^+-ISM electrodes gave comparable E^o stability under a conditioning period of 51 days. This means that when GC-AuNPs was used as conducting substrate, the E^o stability of the K^+-ISE with PEDOT(PSS) as solid-contact is comparable to that with PEDOT(Cl) as solid-contact. Compared to the SC-K^+-ISEs with glassy carbon as conducting substrate, the E^o stability of the SC-K^+-ISEs with GC-AuNPs as conducting substrate were relatively higher.

Solid-contact Cl^--ISEs were also prepared using PEDOT(Cl) and AgCl as solid-contacts and PVC-based Cl^--selective membrane. For the Cl^--ISEs with PEDOT(Cl) as solid-contact, the E^o stability of the SC-Cl^--ISE with glassy carbon as the conducting substrate was compared to that with GC-AuNPs as conducting substrate. The results showed that the E^o stability was higher for the SC-Cl^--ISE with GC-AuNPs as the conducting substrate than that with GC as conducting substrate, from calibrations carried out after 6 days of conditioning. The entire conditioning period was 28 days. On the other hand, the Ag/AgCl/Cl^--ISM electrode gave a comparable E^o stability to the PEDOT-based SC-Cl^--ISEs for a longer conditioning period of 103 days.

The effect of silver deposition in the PEDOT(PSS) film on the potentiometric response of the GC/PEDOT(PSS) electrode was also studied. Accumulation of silver in the PEDOT(PSS) film was found to occur spontaneously after conditioning in 0.01 M $AgNO_3$. The presence of silver in the polymer film was confirmed by cyclic voltammetry measurements and SEM/EDAX measurements. The GC/PEDOT(PSS) electrode with Ag-deposited PEDOT(PSS) film showed cationic response in $AgNO_3$, Na_2SO_4, NaF, $NaHCO_3$, $Na_2C_2O_4$, KNO_3, and $K_2Cr_2O_7$ solutions. On the other hand, anionic response was observed in KCl, KI, NaBr, and NaSCN solutions. The anionic response may be attributed to the presence of silver in the polymer film which can form a salt with the anions present. Interestingly, the slopes of the calibration curves, in the case of solutions where anionic response was observed, seemed to correlate with the K_{sp} of the salt formed between silver and the anion present. This observation could be subject for further study.

The E^o stability of the GC/PEDOT(PSS)/K^+-ISM electrodes with Ag-deposited PEDOT(PSS) films was also evaluated using repeated calibrations. For the prepared GC/PEDOT(PSS)/K^+-ISM electrodes, the effect of performing cyclic voltammetry on the GC/PEDOT(PSS) electrode after conditioning in $AgNO_3$ was also studied. Better E^o stability was observed for the GC/PEDOT(PSS)/K^+-ISM electrode in which no cyclic voltammogram was recorded for the GC/PEDOT(PSS) than those in which cyclic voltammograms for GC/PEDOT(PSS) were recorded in KCl or KNO_3. On the other hand, there was no significant difference between the E^o stability of the GC/PEDOT(PSS)/K^+-ISM electrode in which cyclic voltammograms were recorded for GC/PEDOT(PSS) in KCl and the one in which cyclic voltammograms were recorded for GC/PEDOT(PSS) in KNO_3. These results suggest that performing cyclic voltammetry on GC/PEDOT(PSS), whether in KCl or in KNO_3, did not improve the E^o stability of GC/PEDOT(PSS)/K^+-ISM electrodes with Ag-deposited PEDOT(PSS) films. Furthermore, silver deposition in the PEDOT(PSS) film did not result in better E^o stability for the GC/PEDOT(PSS)/K^+-ISM electrode.

6. References

[1] J. Bobacka, A. Ivaska and A. Lewenstam, *Electroanalysis,* vol. 15, no. 5-6, pp. 366-374, 2003.

[2] B. Nikolskii and E. Materova, "Solid Contact in Membrane Ion-Selective Electrodes," *Ion-Sel. Electrode Rev. ,* vol. 7, pp. 3-39, 1985.

[3] J. Bobacka, *Anal. Chem.,* vol. 71, pp. 4932-4937, 1999.

[4] E. Lindner and R. Gyurcsányi, *J Solid State Electrochem,* vol. 13, pp. 51-68, 2009.

[5] E. Tolstopyatova, N. Pogulyaichenko and V. Kondratiev, *RUSSIAN JOURNAL OF ELECTROCHEMISTRY ,* vol. 50, no. 6, pp. 510-516, 2014.

[6] X. Zou, J. Cheong, B. Taitt and P. Bühlmann, *Anal. Chem.,* vol. 85, pp. 9350-9355, 2013.

[7] C. Jayakumar, C. Magdalene, K. Kaviyarasu, M. Kulandainathan, B. Jeyaraj and M. Maaza, *Journal of Nanoscience and Nanotechnology,* vol. 18, pp. 1-7, 2018.

[8] K. Mikhelson, Ion-selective electrodes, Springer: Heidelberg, 2013.

[9] International Union of Pure and Applied Chemistry (IUPAC), *Pure & Appl. Chem,* vol. 63, no. 9, pp. 1247-1250, 1991.

[10] B. Eggins, Chemical Sensors and Biosensors, John Wiley & Sons, Ltd, 2002.

[11] J. Bobacka, A. Ivaska and A. Lewenstam, *Chem. Rev.,* vol. 108, pp. 329-351, 2008.

[12] J. Wang, Analytical Electrochemistry, John Wiley & Sons, Inc., 2006.

[13] D. Skoog, D. West, F. Holler and S. Crouch, Fundamentals of Analytical Chemistry pp. 595-607, 2004.

[14] D. C. Harris, Quantitative Chemical Analysis pp 321, W. H. Freeman and Company, 2007.

[15] R. Cattrall and I. Hamilton, in *Ion-Sel. Electrode Rev. 6*, 1984, p. 125.

[16] J. Bobacka, *Electroanalysis,* vol. 18, pp. 7-18, 2006.

[17] P. Buhlmann, E. Pretsch and E. Bakker, *Chem. Rev.,* vol. 98, pp. 1593-1687, 1998.

[18] G. Inzelt, Conducting Polymers, Berlin: Springer-Verlag, 2008.

[19] D. Wise, G. Wnek, D. Trantolo, T. Cooper and J. Gresser, Electrical and Optical Polymer Systems, New York: Marcel Dekker Inc., 1998.

[20] A. Heeger, Synth. Met. 125, 2002.

[21] J. Bobacka, A. Lewenstam and A. Ivaska, *Journal of Electroanalytical Chemistry,* vol. 489, pp. 17-27, 2000.

[22] L. Groenendaal, F. Jonas, D. Freitag, H. Pielartzik and J. Reynolds, *Adv. Mater.,* vol. 12, no. 7, pp. 481-494, 2000.

[23] M. Vázquez, J. Bobacka, A. Ivaska and A. Lewenstam, *Sensors and Actuators,* vol. 82, pp. 7-13, 2002.

[24] U. Spichiger-Keller, "Chemical Sensors and Biosensors for Medical and Biological Applications," Weinheim, Wiley-VCH, 1998, p. 161.

[25] E. Bakker and E. Pretsch, *Anal. Chim. Acta,* vol. 309, pp. 7-17, 1995.

[26] D. Ammann, E. Pretsch and W. Simon, *Anal. Chim. Acta,* vol. 171, pp. 119-129, 1985.

[27] J. Janata, Principles of Chemical Sensors 2nd ed., New York: Springer, 2009.

[28] P. Buhlmann and L. Chen, in *Supramolecular Chemistry: From Molecules to Nanomaterials*, John Wiley & Sons, 2012, pp. 2539-2579.

[29] G. Rumpf, U. Spichiger-Keller, H. Buhler and W. Simon, *Analytical Sciences,* vol. 8, pp. 553-559, 1992.

[30] J. Hu, A. Stein and P. Buhlmann, *Trends in Analytical Chemistry,* vol. 76, pp. 102-114, 2016.

[31] U. Vanamo, *Solid-state Reference and Ion-selective Electrodes - Towards Portable Potentiometric Sensing. Acad. Dissert.,* Åbo Akademi University, Turku, Finland, 2015.

[32] A. Lewenstam, J. Bobacka and A. Ivaska, *J. Electroanal. Chem.,* vol. 368, pp. 23-31, 1994.

[33] A. Heeger, S. Sariciftci and E. Namdas, Semiconducting and Metallic Polymers, Oxford, New York: Oxford University Press, 2010.

[34] Z. Mousavi, J. Bobacka, A. Lewenstam and A. Ivaska, *J. Electroanal. Chem.,* vol. 633, pp. 246-252, 2009.

[35] M. Fibbioli, W. Morf, M. Badertscher, N. De Rooij and E. Pretsch, *Electroanalysis,* vol. 12, pp. 1286-1292, 2000.

[36] M. Vázquez, P. Danielsson, J. Bobacka, A. Lewenstam and A. Ivaska, *Sensors and Actuators,* vol. 97, pp. 182-189, 2004.

[37] R. Gyurcsányi, N. Rangisetty, S. Clifton, B. Pendley and E. Lindner, *Talanta,* vol. 63, pp. 89-99, 2004.

[38] T. Lindfors, L. Höfler, G. Jagerszki and R. Gyurcsanyi, *Analytical Chemistry,* vol. 83, pp. 4902-4908, 2011.

[39] Z. Mousavi, J. Bobacka and A. Ivaska, *Electroanalysis,* vol. 17, pp. 1609-1615, 2005.

[40] M. Guzinski, J. Jarvis, B. Pendley and E. Lindner, *Anal. Chem. ,* vol. 87, pp. 6654-6659, 2015.

[41] J. Cazes, Ewing's Analytical Instrumentation Handbook 3rd ed., New York: Marcel Dekker, 2005.

[42] J. Koryta, J. Dvorak and L. Kavan, Principles of Electrochemistry, 2nd ed., Chichester, U.K.: Wiley, 1993.

[43] Z. Mousavi, J. Bobacka, A. Lewenstam and A. Ivaska, *J. Electroanal. Chem.,* vol. 593, pp. 219-226, 2006.

[44] P. Sjöberg-Eerola, J. Bobacka, A. Lewenstam and A. Ivaska, *Sensors and Actuators ,* vol. B 127, pp. 545-553, 2007.

[45] R. Zielińska, E. Mulik, A. Michalska, S. Achmatowicz and M. Maj-Żurawska, *Anal. Chim. Acta,* vol. 451, pp. 243-249, 2002.

[46] P. Sjöberg-Eerola, J. Bobacka, T. Sokalski, J. Mieczkowski, A. Ivaska and A. Lewenstam, *Electroanalysis,* vol. 16, no. 5, pp. 379-385, 2004.

[47] Z. Mousavi, K. Granholm, T. Sokalski and A. Lewenstam, *Sensors & Actuators,* vol. 207, pp. 895-899, 2015.

[48] Z. Mousavi, T. Alaviuhkola, J. Bobacka and R. Latonen, *Electrochimica Acta,* vol. 53, pp. 3755-3762, 2008.

[49] M. Vazquez, J. Bobacka, M. Luostarinen, K. Rissanen, A. Lewenstam and A. Ivaska, *J Solid State Electrochem,* vol. 9, pp. 312-319, 2005.

7. Appendix

Appendix A. Cyclic voltammograms of GC/PEDOT(PSS) and GC/PEDOT(Cl) electrodes recorded in 0.1 M KCl.

GC/PEDOT(PSS)
3 replicates labelled A1, A2 and A3

GC/PEDOT(Cl)
3 replicates labelled B1, B2 and B3

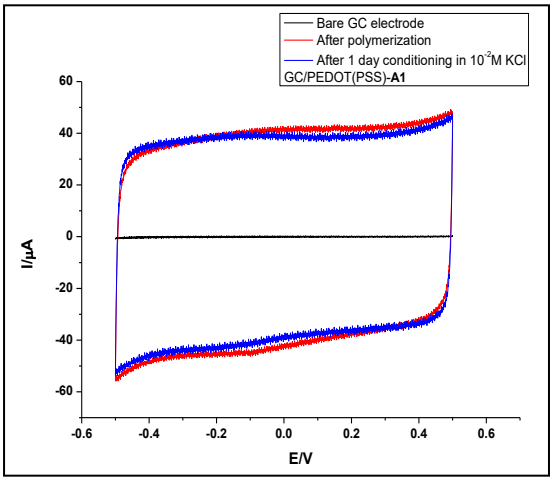

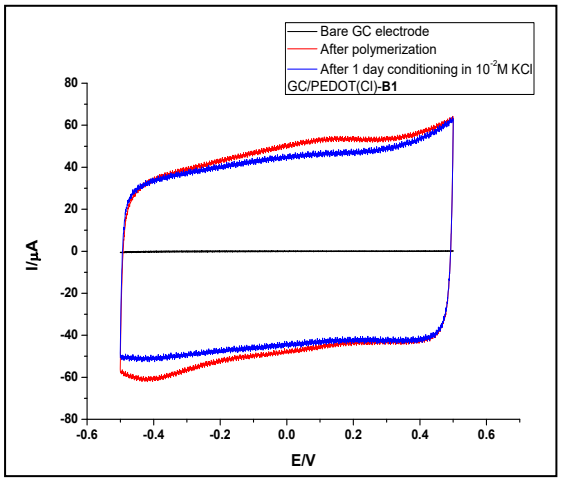

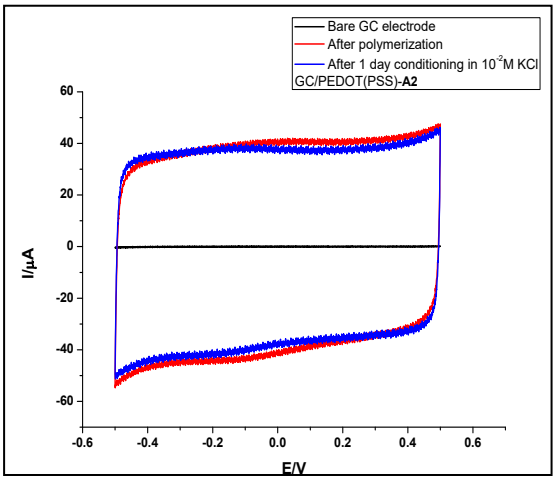

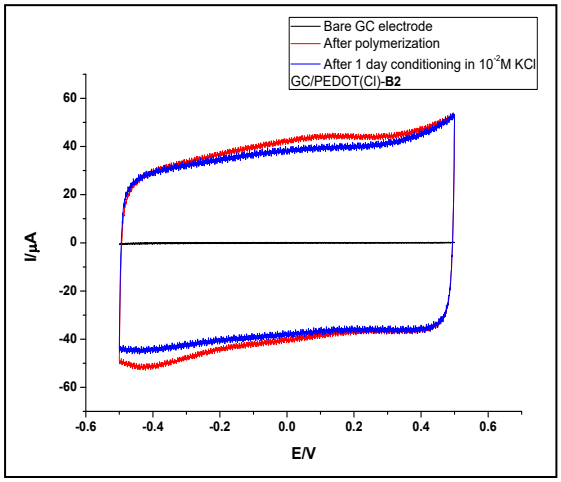

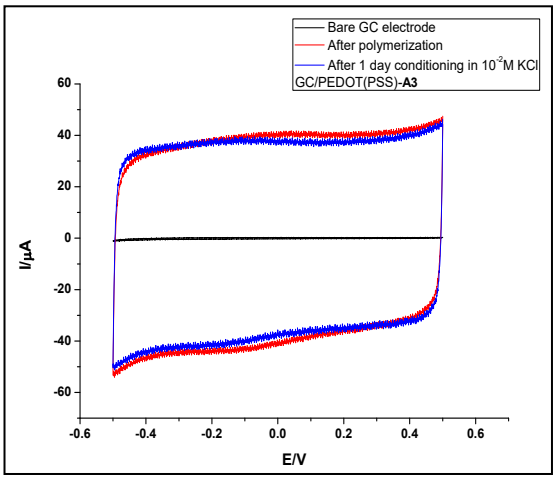

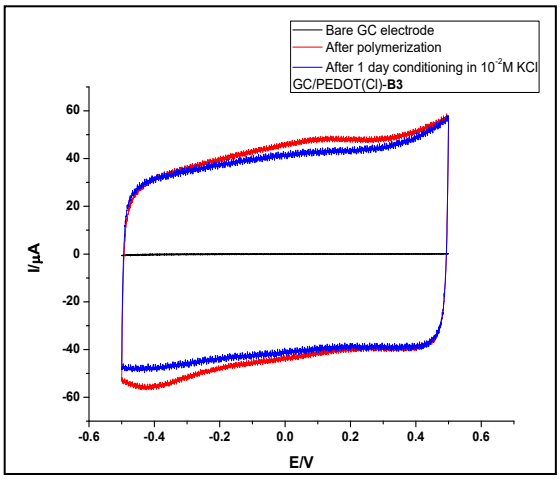

Appendix B. Cyclic voltammograms of GC/PEDOT(PSS) electrodes conditioned in 10^{-2} M $AgNO_3$.

Recorded in 0.1 M KCl | **Recorded in 0.1 M KNO_3**

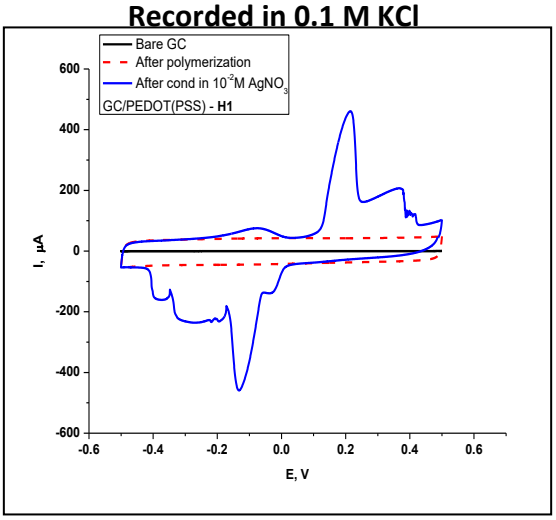

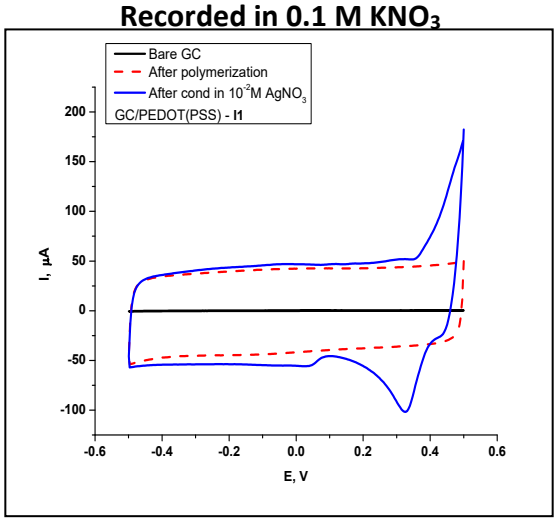

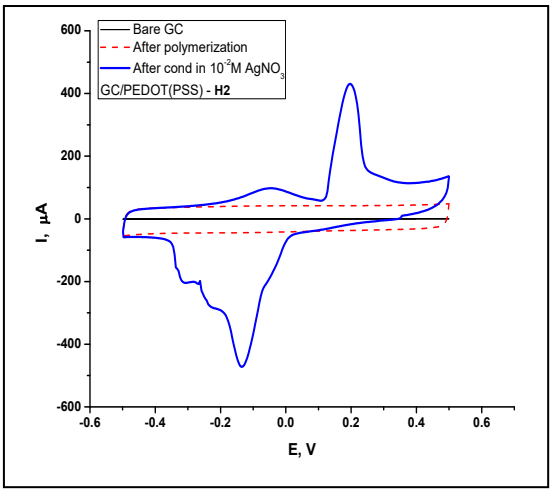

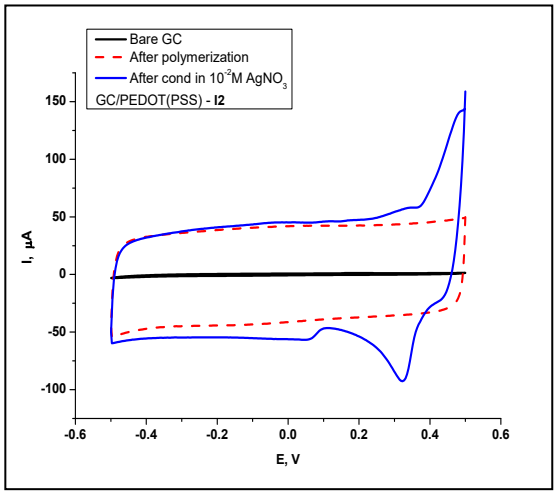

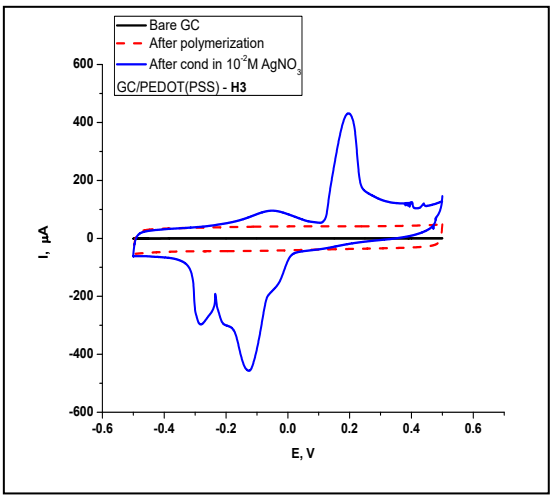

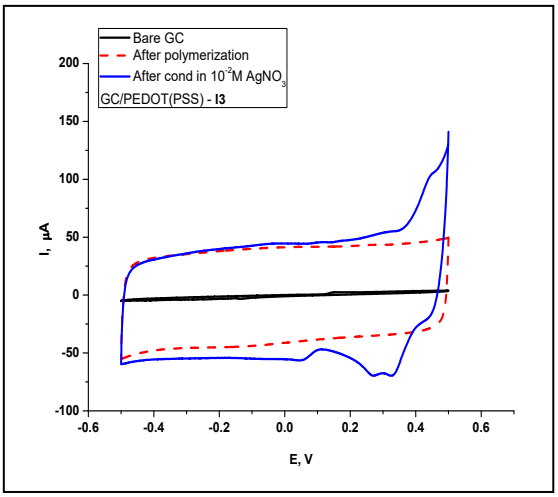

Appendix C. Characterization of GC/PEDOT(PSS), GC/PEDOT(Cl), GC-AuNPs/PEDOT(PSS), and GC-AuNPs/PEDOT(Cl) before and after K^+-ISM application

Table 11. Potentiometric data of GC/PEDOT(PSS), GC/PEDOT(Cl), GC-AuNPs/PEDOT(PSS), and GC-AuNPs/PEDOT(Cl) electrodes and low-frequency capacitance (C_{LF}) estimated from EIS.

Electrode	E^o (mV)	slope (mV/dec)	C_{LF} (µF)
GC/PEDOT(PSS)			
Trial 1	205.1 ± 7.9	49.4 ± 1.2	325
Trial 2	204.8 ± 7.4	49.8 ± 1.4	315
Trial 3	204.8 ± 6.8	49.8 ± 1.1	312
GC/PEDOT(Cl)			
Trial 1	50.0 ± 1.4	-52.3 ± 1.2	364
Trial 2	53.3 ± 0.5	-53.0 ± 1.2	311
Trial 3	53.6 ± 1.6	-53.0 ± 1.0	337
GC-AuNPs/PEDOT(PSS)			
Trial 1	235.7 ± 3.6	48.4 ± 0.4	410
Trial 2	231.0 ± 4.8	47.7 ± 0.3	408
Trial 3	220.8 ± 1.1	44.4 ± 1.0	424
GC-AuNPs/PEDOT(Cl)			
Trial 1	--	--	355
Trial 2	--	--	363
Trial 3	--	--	365

Table 12. Bulk resistance, potential drift, and low-frequency capacitance (C_{LF}) of GC/PEDOT(PSS)/K^+-ISM, GC/PEDOT(Cl)/K^+-ISM, GC-AuNPs/PEDOT(PSS)/K^+-ISM, and GC-AuNPs/PEDOT(Cl)/K^+-ISM electrodes estimated from chronopotentiometry.

Electrode	Bulk Resistance, MΩ	Potential drift, $\Delta E/\Delta t$ (µV/s)	C_{LF} (µF)
GC/PEDOT(PSS)/K-ISM			
Trial 1	4.8	7.7	130
Trial 2	4.0	9.2	108
Trial 3	4.4	8.3	120
GC/PEDOT(Cl)/K-ISM			
Trial 1	4.6	8.2	122
Trial 2	4.3	10.4	96
Trial 3	4.0	9.1	110
GC-AuNPs/PEDOT(PSS)/K-ISM			
Trial 1	4.7	5.5	182
Trial 2	3.8	7.6	132
Trial 3	3.6	7.8	128
GC-AuNPs/PEDOT(Cl)/K-ISM			
Trial 1	4.1	5.9	169
Trial 2	4.2	8.7	115
Trial 3	4.0	8.3	120

Appendix D. Characterization of GC/PEDOT(Cl), GC-AuNPs/PEDOT(Cl), and Ag/AgCl before and after Cl^--ISM application

Table 13. Potentiometric data of GC/PEDOT(Cl), GC-AuNPs/PEDOT(Cl), and Ag/AgCl electrodes and low-frequency capacitance (C_{LF}) estimated from EIS.

Electrode	E^o (mV)	slope (mV/dec)	C_{LF} (µF)
GC/PEDOT(Cl)			
Trial 1	77.2 ± 1.7	-52.1 ± 0.2	307
Trial 2	81.7 ± 3.2	-47.6 ± 0.1	322
Trial 3	81.0 ± 1.5	-49.5 ± 0.3	315
Ag/AgCl			
Trial 1	28.8 ± 1.4	-54.9 ± 0.6	--
Trial 2	28.3 ± 1.3	-55.1 ± 0.6	--
Trial 3	33.0 ± 0.8	-54.5 ± 0.4	--
GC-AuNPs/PEDOT(Cl)			
Trial 1	--	--	363
Trial 2	--	--	382
Trial 3	--	--	368

Table 14. Bulk resistance, potential drift, and low-frequency capacitance (C_{LF}) of GC/PEDOT(Cl)/Cl-ISM, and GC-AuNPs/PEDOT(Cl)/Cl-ISM electrodes estimated from chronopotentiometry.

Electrode	Bulk Resistance, MΩ	Potential drift, $\Delta E/\Delta t$ (µV/s)	C_{LF} (µF)
GC/PEDOT(Cl)/Cl-ISM			
Trial 1	155	4.6	217
Trial 2	135	3.3	303
Trial 3	165	3.3	303
GC-AuNPs/PEDOT(Cl)/Cl-ISM			
Trial 1	120	3.7	270
Trial 2	135	3.5	284
Trial 3	150	3.3	304

Appendix E. Calibration data of the fabricated K^+-ISEs during different days of conditioning in 0.01 M KCl.

Table 15. Calibration data of GC/PEDOT(PSS)/K^+-ISM, GC/PEDOT(Cl)/K^+-ISM, and a commercial K^+-ISE during different days of conditioning in 0.01 M KCl

Electrode	Days of conditioning														Average*	Std. Deviation*
	3	4	8	9	10	11	28	35	42	49	57	74	79	103		
GC/PEDOT(PSS)/K-ISM																
Trial 1																
Slope	56.61	56.82	56.80	57.14	56.50	57.04	56.88	56.81	55.25	56.23	56.02	56.05	56.16	56.60	**56.34**	**0.56**
Intercept	236.69	234.30	240.02	243.69	242.96	237.88	251.40	255.04	258.08	264.59	267.22	269.38	261.67	262.33	**257.06**	**9.64**
Trial 2																
Slope	57.37	57.26	57.71	58.18	57.11	58.27	53.25	53.05	50.46	52.44	53.86	53.94	53.21	55.99	**53.83**	**2.21**
Intercept	277.25	274.37	284.80	287.97	286.70	283.44	295.15	305.54	308.09	317.45	325.95	334.92	320.28	334.30	**311.18**	**17.46**
Trial 3																
Slope	57.61	57.31	57.86	58.03	57.25	58.53	59.17	58.52	56.54	58.22	57.87	58.60	58.26	58.86	**58.29**	**0.75**
Intercept	246.53	243.95	252.56	254.63	253.73	250.42	270.68	277.23	279.32	290.10	295.35	305.34	298.25	306.53	**282.70**	**18.28**
GC/PEDOT(Cl)/K-ISM																
Trial 1																
Slope	57.46	57.42	57.95	58.12	57.10	58.62	59.10	58.40	56.53	58.19	58.01	58.77	58.17	59.15	**58.33**	**0.79**
Intercept	279.59	279.77	296.00	297.85	298.23	295.44	318.60	315.61	315.47	322.82	322.98	324.93	317.45	322.41	**315.39**	**8.89**
Trial 2																
Slope	57.73	57.42	56.23	56.80	56.13	57.10	56.70	57.07	55.41	56.43	56.13	57.22	56.63	57.00	**56.63**	**0.58**
Intercept	279.11	279.77	288.16	291.16	289.61	282.92	278.24	282.83	276.84	281.90	281.20	293.29	284.02	281.93	**283.28**	**4.63**
Trial 3																
Slope	57.38	57.42	57.98	58.03	57.16	58.68	59.13	58.47	56.27	58.36	58.01	58.88	58.21	59.41	**58.38**	**0.91**
Intercept	319.23	320.34	330.49	331.51	330.33	326.47	341.47	347.67	348.69	360.43	360.20	366.37	356.49	361.96	**350.01**	**12.53**
Commercial K-ISE																
Slope	--	--	56.89	56.88	56.16	56.26	57.94	54.96	56.84	57.36	57.45	58.10	56.72	57.68	**57.03**	**0.98**
Intercept	--	--	98.05	99.71	96.97	85.38	88.75	86.77	90.35	92.45	92.79	93.30	84.58	83.19	**89.45**	**3.82**

* for data taken after 10 days of conditioning

Table 16. Calibration data of GC-AuNPs/PEDOT(PSS)/K^+-ISM, GC-AuNPs/PEDOT(Cl)/K^+-ISM and a commercial K^+-ISE during different days of conditioning in 0.01 M KCl.

Electrode	Days of conditioning									Average*	Std. Deviation*
	4	**6**	**8**	**15**	**22**	**29**	**32**	**42**	**51**		
GC-AuNPs/PEDOT(PSS)/K-ISM											
Trial 1											
Slope	56.94	58.69	58.52	58.67	59.00	58.14	59.11	56.92	57.11	**58.16**	**0.95**
Intercept	311.56	319.59	326.35	337.78	341.02	336.37	339.83	336.10	340.96	**338.68**	**2.23**
Trial 2											
Slope	56.97	58.45	58.37	58.44	59.08	58.11	59.28	58.27	56.95	**58.36**	**0.83**
Intercept	302.74	311.34	317.83	331.62	338.45	336.35	341.72	345.71	348.44	**340.38**	**6.19**
Trial 3											
Slope	57.05	58.67	58.53	58.38	58.67	58.10	59.28	57.81	57.09	**58.22**	**0.75**
Intercept	289.69	298.28	303.88	313.63	316.48	310.38	312.84	310.34	300.44	**310.69**	**5.51**
GC-AuNPs/PEDOT(Cl)/K-ISM											
Trial 1											
Slope	57.13	58.94	58.50	58.84	59.00	58.37	59.11	58.03	56.76	**58.35**	**0.88**
Intercept	281.72	290.63	295.36	307.15	312.48	311.10	314.90	318.93	323.76	**314.72**	**5.91**
Trial 2											
Slope	57.31	57.81	58.26	58.81	59.16	58.17	57.87	57.89	56.43	**58.06**	**0.95**
Intercept	272.50	278.31	285.69	301.29	311.03	310.26	311.87	320.04	322.57	**312.84**	**7.63**
Trial 3											
Slope	57.35	58.78	58.83	58.80	59.11	58.22	58.70	57.91	56.83	**58.26**	**0.82**
Intercept	303.29	310.64	316.94	330.55	336.78	334.28	337.01	337.83	337.18	**335.61**	**2.76**
Commercial K-ISE											
Slope	56.95	57.70	57.51	57.87	58.38	56.46	55.53	57.36	55.60	**57.04**	**1.19**
Intercept	91.12	92.91	92.91	93.47	93.52	82.84	82.81	82.96	82.48	**88.34**	**5.54**

*for data taken after 10 days of conditioning

Appendix F. Calibration data of the fabricated Cl^--ISEs during different days of conditioning in 0.01 M KCl.

Table 17. Calibration data of Ag/AgCl/Cl^--ISM and a commercial Cl-ISE during different days of conditioning in 0.01 M KCl.

Electrode	Days of conditioning														Average*	Std. Deviation*
	3	4	8	9	10	11	28	35	42	49	57	74	79	103		
Ag/AgCl/Cl-ISM																
Trial 1																
Slope	-50.38	-52.45	-53.34	-53.60	-53.38	-52.41	-53.21	-51.85	-53.06	-54.06	-54.46	-54.31	-54.78	-53.84	**-53.53**	**0.85**
Intercept	41.80	37.55	35.22	33.20	35.15	31.75	26.27	29.03	29.57	29.63	29.75	30.77	24.02	24.16	**29.88**	**3.72**
Trial 2																
Slope	-50.98	-52.18	-53.48	-52.94	-53.06	-51.82	-53.75	-51.90	-53.72	-54.25	-54.27	-54.19	-54.98	-54.05	**-53.53**	**0.96**
Intercept	39.05	37.18	34.02	33.94	35.11	32.15	25.74	29.06	28.69	29.47	30.28	30.60	23.13	23.18	**29.61**	**4.00**
Trial 3																
Slope	-52.22	-53.25	-53.69	-52.62	-53.44	-52.43	-53.84	-50.89	-51.98	-53.64	-52.96	-53.58	-53.84	-53.50	**-53.03**	**0.91**
Intercept	39.58	37.07	34.94	35.42	35.52	32.30	27.00	31.42	32.11	30.30	32.71	31.63	25.47	24.24	**31.09**	**3.75**
Commercial Cl-ISE																
Slope	--	--	-54.68	--	--	--	-55.63	-54.27	-54.72	-54.83	--	-54.49	-55.64	-54.50	**-54.85**	**0.52**
Intercept	--	--	27.39	--	--	--	19.44	21.76	24.48	25.70	--	26.51	18.43	19.23	**22.87**	**3.59**

*for data taken after 6 days of conditioning

Table 18. Calibration data of GC/PEDOT(Cl)/Cl^--ISM, GC-AuNPs/PEDOT(Cl)/Cl^--ISM, and a commercial Cl-ISE during different days of conditioning in 0.01 M KCl.

Electrode	Days of conditioning								Average*	Std. Deviation*
	2	4	6	9	16	19	23	28		
GC/PEDOT(Cl)/Cl-ISM										
Trial 1										
Slope	-50.44	-50.42	-52.82	-52.06	-51.86	-51.97	-52.31	-51.01	-51.84	0.49
Intercept	145.71	115.20	100.50	95.28	89.75	88.06	89.07	93.14	91.06	3.03
Trial 2										
Slope	-50.62	-51.22	-54.97	-53.88	-52.81	-53.47	-52.76	-53.83	-53.35	0.54
Intercept	140.34	84.56	60.42	50.03	43.27	41.78	45.29	47.61	45.60	3.31
Trial 3										
Slope	-50.37	-50.25	-55.10	-53.18	-52.45	-52.64	-52.91	-52.34	-52.70	0.34
Intercept	137.66	80.41	55.36	47.50	43.09	43.13	45.22	51.36	46.06	3.47
GC-AuNPs/PEDOT(Cl)/Cl-ISM										
Trial 1										
Slope	-50.41	-50.89	-52.23	-51.93	-51.26	-52.21	-52.44	-52.18	-52.00	0.45
Intercept	134.07	95.44	85.48	81.16	83.97	81.65	81.59	82.93	82.26	1.16
Trial 2										
Slope	-48.65	-49.99	-52.15	-50.90	-50.60	-52.91	-52.60	-52.31	-51.86	1.04
Intercept	150.53	116.71	103.25	99.20	102.07	96.03	97.18	98.09	98.51	2.30
Trial 3										
Slope	-48.49	-49.88	-51.82	-51.02	-50.58	-50.81	-51.81	-51.06	-51.06	0.46
Intercept	146.17	100.80	89.59	85.63	89.88	88.08	87.66	90.64	88.38	1.97
Commercial Cl-ISE										
Slope	-54.73	-55.60	-55.43	-54.46	--	--	-54.27	-54.50	-54.41	0.12
Intercept	27.24	18.48	17.85	19.17	--	--	18.68	19.23	19.03	0.30

*for data taken after 6 days of conditioning

Appendix E. Elemental composition of different Pt/PEDOT(PSS) films conditioned in 0.01 M KCl or 0.01 M $AgNO_3$

Table 19. Elemental composition of different types of Pt/PEDOT(PSS) films obtained from EDAX.

Type of Pt/PEDOT(PSS) film	Elements present, % wt.					
	C	O	S	Al	N	Ag
Control - no conditioning	43.48 ± 1.20	41.60 ± 0.58	10.79 ± 0.27	4.13 ± 0.12		
Conditioned in 0.01 M KCl - No CV recorded						
Trial 1	46.10 ± 1.32	45.03 ± 0.84	7.53 ± 0.43	1.34 ± 0.21		
Trial 2	47.50 ± 1.31	44.18 ± 0.75	6.73 ± 0.38	1.59 ± 0.19		
Conditioned in 0.01 M $AgNO_3$ - No CV recorded						
Trial 1	30.60 ± 0.94	40.66 ± 0.81	6.41 ± 0.28	2.46 ± 0.13	18.26 ± 2.81	1.62 ± 0.19
Trial 2	33.87 ± 1.05	38.84 ± 0.91	7.76 ± 0.34	1.81 ± 0.16	11.58 ± 2.37	6.14 ± 0.27
Conditioned in 0.01 M $AgNO_3$ - CV recorded in KCl						
Trial 1	29.22 ± 0.97	40.44 ± 0.84	6.06 ± 0.29	1.99 ± 0.15	18.93 ± 2.83	2.90 ± 0.41
Trial 2	29.77 ± 0.93	40.23 ± 0.73	6.07 ± 0.24	1.13 ± 0.12	18.70 ± 2.40	4.12 ± 0.34
Conditioned in 0.01 M $AgNO_3$ - CV recorded in KNO_3						
Trial 1	26.73 ± 0.90	39.01 ± 0.85	5.23 ± 0.29	1.82 ± 0.15	16.28 ± 2.53	10.93 ± 0.47
Trial 2	26.56 ± 0.94	39.78 ± 1.01	4.97 ± 0.34	0.91 ± 0.18	18.99 ± 2.93	8.78 ± 0.54

Appendix F. Calibration data of GC/PEDOT(PSS) electrodes conditioned in 0.01 M $AgNO_3$ in different electrolyte solutions.

Table 20. Calibration data of GC/PEDOT(PSS) electrodes conditioned in 0.01 M $AgNO_3$ in solutions where cationic response was observed.

Electrode	Calibration in $AgNO_3$		Calibration in KNO_3		Calibration in $K_2Cr_2O_7$		Calibration in $Na_2C_2O_4$		Calibration in $NaHCO_3$		Calibration in Na_2SO_4		Calibration in NaF	
	E^o (mV)	slope (mV/dec)	E^o (mV)	slope (mV/dec)	E^o (mV)	slope (mV/dec)	E^o (mV)	slope (mV/dec)	E^o (mV)	slope (mV/dec)	E^o (mV)	slope (mV/dec)	E^o (mV)	slope (mV/dec)
GC/PEDOT(PSS) - No CV recorded														
Trial 1	573.1 ± 3.4	51.3 ± 1.8	358.7	46.0	567.5	43.6	358.6	41.1	351.7	48.0	342.9	42.4	343.1	48.2
Trial 2	575.2 ± 2.6	52.6 ± 1.0	361.0	46.7	570.0	43.7	359.3	44.3	357.5	49.8	337.2	42.6	345.6	48.5
Trial 3	573.4 ± 2.1	51.3 ± 1.5	--	--	--	--	--	--	--	--	--	--	--	--
GC/PEDOT(PSS) - CV recorded in 0.1 M KCl														
Trial 1	580.0 ± 0.8	53.2 ± 0.7	355.9	45.7	568.7	41.9	353.6	39.4	357.0	47.6	337.3	43.3	337.9	48.3
Trial 2	579.4 ± 2.3	52.2 ± 0.2	359.1	45.7	569.5	45.6	357.6	40.6	356.6	47.2	340.5	43.6	349.3	49.3
Trial 3	579.9 ± 0.4	51.8 ± 1.0	--	--	--	--	--	--	--	--	--	--	--	--
GC/PEDOT(PSS) - CV recorded in 0.1 M KNO_3														
Trial 1	577.3 ± 1.8	52.5 ± 0.5	350.4	36.2	573.7	46.7	355.6	42.0	355.8	46.4	343.1	42.1	346.3	47.0
Trial 2	575.7 ± 0.9	48.0 ± 0.4	361.7	44.5	572.5	44.3	356.1	39.9	356.6	46.1	339.1	42.4	347.7	47.7
Trial 3	576.4 ± 4.4	49.7 ± 1.0	--	--	--	--	--	--	--	--	--	--	--	--

Table 21. Calibration data of GC/PEDOT(PSS) electrodes conditioned in 0.01 M $AgNO_3$ in solutions where cationic response was observed.

Electrode	Calibration in KCl		Calibration in NaBr		Calibration in KI		Calibration in NaSCN	
	E^o (mV)	slope (mV/dec)	E^o (mV)	slope (mV/dec)	E^o (mV)	slope (mV/dec)	E^o (mV)	slope (mV/dec)
GC/PEDOT(PSS) - No CV recorded								
Trial 1	41 ± 12	-46.9 ± 3.1	-116.4	-46.0	-248.2	-22.7	-77.2	-41.5
Trial 2	39 ± 7	-47.4 ± 1.8	-111.3	-43.9	-261.0	-26.4	-75.2	-39.9
Trial 3	28.5 ± 0.6	-51.3 ± 0.4	--	--	--	--	--	--
GC/PEDOT(PSS) - CV recorded in 0.1 M KCl								
Trial 1	29 ± 2	-50.9 ± 0.8	-119.8	-47.8	-271.8	-30.7	-72.9	-38.7
Trial 2	28 ± 2	-50.9 ± 0.3	-117.4	-47.4	-262.5	-28.5	-67.1	-38.1
Trial 3	31 ± 4	-49.5 ± 1.1	--	--	--	--	--	--
GC/PEDOT(PSS) - CV recorded in 0.1 M KNO_3								
Trial 1	22 ± 5	-52.9 ± 1.5	-118.0	-47.4	-243.4	-25.0	-71.7	-40.0
Trial 2	33 ± 4	-47.9 ± 1.2	-118.2	-47.3	-251.8	-26.2	-74.9	-40.5
Trial 3	30 ± 3	-49.8 ± 0.8	--	--	--	--	--	--

Appendix G. Calibration data of the GC/PEDOT(PSS)/K^+-ISM electrodes with Ag-deposited PEDOT(PSS) films during different days of conditioning in 0.01 M KCl.

Table 22. Calibration data of different GC/PEDOT(PSS)/K^+-ISM electrodes with Ag-deposited PEDOT(PSS) films and a commercial K^+-ISE during different days of conditioning in 0.01 M KCl.

Electrode	Days of conditioning							Average	Std. Deviation
	5	6	12	16	30	49	73		
GC/PEDOT(PSS)/K-ISM -1									
Trial 1									
Slope	57.46	57.68	56.74	56.90	57.34	57.57	55.74	57.06	0.68
Intercept	202.71	173.26	173.33	175.45	161.17	171.99	184.79	177.53	13.07
Trial 2									
Slope	57.35	57.43	57.24	56.72	58.68	58.81	57.51	57.68	0.77
Intercept	426.82	400.84	399.64	396.91	404.00	387.32	383.51	399.86	14.01
Trial 3									
Slope	57.89	57.65	57.81	57.31	58.85	59.10	57.77	58.05	0.66
Intercept	216.76	222.25	233.23	236.43	250.93	247.94	247.41	236.42	13.30
	Days of conditioning							**Average**	**Std. Deviation**
	3	**9**	**11**	**17**	**22**	**44**	**68**		
GC/PEDOT(PSS)/K-ISM-2									
Trial 1									
Slope	57.96	58.19	58.38	58.12	57.80	59.32	59.74	58.50	0.74
Intercept	385.08	362.42	359.05	349.97	344.51	327.13	316.06	349.17	22.97
Trial 2									
Slope	58.11	58.58	58.29	58.19	57.76	59.12	59.58	58.52	0.63
Intercept	365.01	340.98	334.12	347.28	311.33	261.16	250.87	315.82	43.98
Trial 3									
Slope	57.92	58.09	58.24	58.18	57.77	59.32	59.72	58.46	0.75
Intercept	374.25	356.33	353.85	320.14	344.29	332.60	302.34	340.54	24.21
GC/PEDOT(PSS)/K-ISM-3									
Trial 1									
Slope	56.96	57.90	57.53	57.61	56.36	56.62	58.36	57.33	0.72
Intercept	360.60	304.89	298.75	288.56	279.19	299.78	293.51	303.61	26.50
Trial 2									
Slope	57.53	57.58	58.24	57.61	56.36	57.35	56.24	57.27	0.72
Intercept	329.76	340.54	339.29	288.56	279.19	191.53	186.98	279.41	66.09
Trial 3									
Slope	58.11	58.54	58.24	57.22	57.35	58.82	59.72	58.29	0.86
Intercept	370.62	343.72	339.29	325.75	322.76	307.99	302.34	330.35	23.25
Commercial K-ISE									
Slope	57.34	57.68	57.71	57.56	56.94	58.08	57.73	57.58	0.36
Intercept	90.06	92.37	91.52	91.52	91.64	87.16	86.34	90.09	2.39